Assessment of Metal Condition and Remaining Life of In-service Power Plant Components Operating at High Temperature

ANDREI DEDOV

TALLINN UNIVERSITY OF TECHNOLOGY
Faculty of Mechanical Engineering
Department of Thermal Engineering

Dissertation was accepted for the defence of the degree of Doctor of Philosophy in Engineering on November 8, 2007

Supervisor: Professor, D.Sc. Ivan Klevtsov, Faculty of Mechanical Engineering

Opponents: Ph.D. Andrey Tugov, All-Russia Thermal Engineering Institute, Moscow, Russia
D.Sc. Priit Kulu, Tallinn University of Technology, Tallinn, Estonia
Ph.D. Tõnu Suurkuusk, Tallinn, Estonia

Defence of the thesis: December 17, 2007

Declaration:
Hereby I declare that this doctoral thesis, my original investigation and achievement, submitted for the doctoral degree at Tallinn University of Technology has not been submitted for any academic degree.

Andrei Dedov

Elektrijaamade kõrgetemperatuursete seadmete metalli seisundi ja jääkressursi hindamine

ANDREI DEDOV

Table of Contents

INTRODUCTION

Motivation of the study

One of the most important missions in the heat-and-power engineering is increasing the durability and operating reliability of new components of power equipment as well as components that had exceeded the nominal design life. Boilers and turbines of Narva Power Plants in Estonia were designed for 200 thousands hours of operation, but the basic components (except for unit 8 of Eesti Power Plant and unit 11 of Balti Power Plant) have been already in operation for 250 thousands hours up to the present. Nowadays such components of power equipment require continuous and closer control or replacement (if it is needed). In this case in order to increase the durability of power equipment without sacrificing the safety and reliability it is highly significant to test the components experimentally as accurately as possible. It allows to estimate the integrity of the in-service components, assess their remaining life or the life till the next mandatory inspection and make reasonable 3R decisions (run or repair or replacement).

During the operation the components of power plant suffer the material deterioration in terms of strength decrease due to the change in microstructure of the metal caused by long-term operation at high temperatures. The typical degradation mechanisms of the power plant components materials are the creep deformation, thermal fatigue, high temperature corrosion, etc. Therefore, in order to get reliable integrity assessment and remaining life estimation in addition to structural analysis the determination of material properties of a component in-service is required. In order to estimate the mechanical properties the metal sample should be extracted from the actually exposed components. Several methods of metal sampling were developed in recent two decades. However, acceptability of the metal sampling from the in-service components needs to be analysed. The latter consists in stress distribution analysis in the vicinity of the dimple after sampling in order to specify the allowable amount of the extracted sample that allows continued exposure without degrading of integrity of the component and without unallowable increase of stress. As regards the determination of the mechanical properties, many researchers have investigated small specimen testing techniques and one such technique is a small punch test. This method is not yet standardised since the behaviour of the specimen in small punch test is still not fully understood and any ideas to improve, develop and make more reliable the tests are very welcome.

Another dominant factor of material deterioration is high temperature corrosion. Combustion of Estonian oil shale containing inorganic matter produces several chemically active compounds leading to both fouling and accelerated high temperature corrosion of heating surfaces. In spite of the fact, that many of steels have been investigated, the research of high temperature corrosion of different new steels in order to reveal the most corrosion-resistant and most suitable one for operation in the conditions of high temperature corrosion under influence of oil

shale ash deposits is always of high importance. Thus, the tubes of superheater and reheater of oil shale steam boilers are subjected to intensive corrosion, which causes thinning of the tubes wall and increasing of stresses that in turn reduces the creep life of the tubes and could lead to ultimate failure. This requires preventive shutdown of the boilers every 3–4 years for the major overhaul in order to replace up to 30–50% of austenitic tubes in the superheater. Therefore, the ability to predict accurately the remaining life of the heating surfaces tubes subjected to intensive corrosion would help to optimise the schedule of the boilers outages and to reduce expenses of the superheater and reheater tubes replacement.

Thus, an advance in the accuracy improving of the assessment of the power plant components operational integrity allows to reduce the amount and cost of the repair and to avoid unscheduled outages of the equipment and components failures, which can lead to serious injury or even loss of the life for personnel. Therefore, the research in this field is of a vital importance, which cannot be overestimated.

Objectives of the thesis

The evaluation of the metal deterioration degree of the power plant in-service components has been set as an object of this work. The specific objectives have been:

- Applicability analysis of tensile properties determination of power plant steels by means of indirect techniques on the basis of hardness.
- To analyse the impact of the dimple on stress distribution in power plant components with a view to analyse the acceptability of samples extraction from the in-service components without subsequent repair.
- To carry out the small punch tests and to make a finite element model of the punching process in order to analyse the applicability of the method for determination of material tensile properties of the power plant components.
- To develop and to implement the reliable technique for determination of the metal tensile properties by testing of miniature specimens, which can be fabricated from small samples, extracted from the in-service power plant component.
- To carry out laboratory and industrial high temperature corrosion tests of several austenitic steels with the aim to reveal the most suitable one for operation in the conditions of high temperature corrosion under influence of Estonian oil shale ash deposits.
- To develop the technique for the prediction of the remaining life of the steam boilers heating surfaces tubes subjected to high temperature corrosion, cyclic destruction of oxide scale and creep.

7

List of publications

The thesis is based on the following publications, which are referred to in the text by the Roman numerals:

I. Tallermo H., Klevtsov I., Bojarinova T., **Dedov A.** Laboratory tests of high temperature corrosion of steels B-407, X8CrNiNb1613 and X8CrNiMoNb1616 under impact of PF oil shale ash. Oil Shale, 2005, Vol. 22, No. 4S, pp. 467–474.

II. Tallermo H., Klevtsov I., Bojarinova T., **Dedov A.** Assessment of Remaining Life of Superheater austenitic Steel Tubes in PF Oil Shale Boilers. Oil Shale, 2006, Vol. 23, No. 3, pp. 267–274.

III. **Dedov A.**, Klevtsov I., Lausmaa T., Neshumayev D. Method of small samples for assessment of properties of power plant components: sampling devices and stress concentration in dimples. *In:* Proceedings of international conference Baltica VII on Life Management and Maintenance for Power Plants, Helsinki – Stockholm – Helsinki, 12–14 June, 2007, Vol. 2. Helsinki: VTT Technical Research Centre of Finland, pp. 180–192.

IV. Klevtsov I., **Dedov A.**, Bogolyubova E., Bojarinova T. Significance of direct testing of mechanical properties of power equipment metal. Accepted for publication in Thermal Engineering (in Russian).

The personal contribution of the author

The contribution by the author to the papers included in the thesis is as follows:

I Major role in writing. Data reduction. Analysis and discussion of the results.

II Major role in writing. The author has suggested the method of remaining life assessment of superheater tubes subjected to intensive high temperature corrosion.

III Minor role in writing. Participating in metal sampling from in-service power plant components. Finite element modelling of the dimple on the surface of the components and stress distribution analysis in the sampled area. Analysis and discussion of the results.

IV Major role in writing. Collecting, analysis and discussion of data.

The author has made a finite element model of the punch process for simulation of small punch test. The author has directly taken part in small punch testing of disk-shaped specimens and tensile testing of miniature flat specimens and in discussion of the obtained results.

The subject of the defence

- Applicability of extraction of small samples from the in-service power plant components.

- Verification and development of the method of small punch testing for determination of tensile properties.
- Verification and development of the miniature flat specimens technique for determination of tensile properties of post-exposed metal of power plant steels.
- Method for estimation of remaining life of steam boiler superheater tubes.
- Application of yield strength and tensile strength of the metal determined in short-term testing at room temperature for integrity and remaining life assessment of in-service power plant components operated in the range of creep.

Scientific novelty of the study

- The technique of the metal tensile properties determination by testing of miniature flat specimens, which can be fabricated from small samples, extracted from the in-service power plant components, is developed and implemented.
- The method for estimation of remaining life of steam boiler superheater tubes operated in conditions of creep, high temperature corrosion and cyclic destruction of metal oxide scale is proposed.

Practical significance of the thesis

The techniques, which have been developed within the present work, are successfully implemented for integrity assessment of the in-service components of Estonian power plants and included into code of practice for metal control of power equipment that is valid in Narva power plants. The method of metal mechanical properties determination is certified by Estonian Accreditation Centre. It makes the thesis to be highly significant and valuable.

Approval of the results

The results of this work were presented in:
- The 5th International Conference of DAAAM "Baltic Industrial Engineering – Adding Innovation Capacity of Labour Force and Entrepreneur", Tallinn, Estonia, 20–22 April, 2006.
- Scientific and Technical Conference "Metal of Thermal Power Plant Equipment. Problems and Perspectives", VTI, Moscow, Russia, 30 October – 02 November, 2006.
- International Conference Baltica VII, "Life Management and Maintenance for Power Plants", Helsinki – Stockholm – Helsinki, 12–14 June, 2007.

SYMBOLS AND ABBREVIATIONS

Roman symbols

A	empirical constant in (Eq. 1.1) and percent elongation of the specimen in Table 2.4, %
B	coefficient expressing corrosive intensity in the initial period
C	empirical constant
D_i	inside diameter of the tube, mm
E	Young's modulus, N/mm^2
f	design stress, N/mm^2
L_0	gauge length of the specimen, mm
m	number of periodic destructions of the oxide scale
n	corrosion rate factor
p	pressure, Pa
P_{LM}	Larson-Miller parameter
P_{max}	maximum punch force in small punch test, N
P_y	force corresponded to the limit of elastic regime and initialization of plastic deformation in small punch test, N
Q	activation energy for the creep process, J/mol
R	universal gas constant, J/(mol·K)
R_e	proportionality limit, N/mm^2
R_m	tensile strength, N/mm^2
$R_{p0.2}$	offset yield strength (proof strength) at 0.2% strain, N/mm^2
S	minimum required wall thickness, mm
S_0	cross area of the gauge section of the specimen, mm^2 and initial thickness of the tube wall in (Eq. 3.7), mm
ΔS	corrosion depth, mm
$\Delta S'$	corrosion depth under the layer of a stable ash deposits, mm
$\Delta S_{allowable}$	allowable reduction of wall thickness, mm
ΔS_o	corrosion depth on the outside surface of the tube, mm
ΔS_i	corrosion depth on the inside surface of the tube, mm
ΔS_{igc}	intergranular corrosion depth, mm
T	absolute temperature, K
z	joint coefficient

Greek symbols

α	empirical constant
β	empirical constant
γ	empirical constant
ε	empirical constant

μ	friction coefficient
ν	Poisson's ratio
ξ	degree of oxide scale destruction
τ	time, h

Abbreviations

ABI	Automated Ball Indentation
EDM	Electro Discharge Machining
CBN	Carbon Boron Nitride
FE	Finite Element
HB	Brinell Hardness
HTC	High Temperature Corrosion
MSM	Mechanical Sampling Machine
NVM	None-Volatile Memory
rpm	rotations per minute
SP	Small Punch

1. THE EFFECT OF THE SERVICE TIME ON THE METAL PROPERTIES AT HIGH TEMPERATURE

The condition assessment for an ageing plant is of primary importance to ensure continued, safe and cost-effective operation. The basic components of power plants are operated under severe conditions such as high temperature and high pressure for a long period of time. Long-term exposure in such conditions causes inevitable degradation of the structure and properties of the materials used in power plants. The deterioration of the material properties leads to the decrease of the power equipment components durability. Therefore in order to increase the operating integrity and reliability of the power equipment it is highly significant to know the potential mechanisms of damage, which can take place during operation and to be able to estimate the state of damage or life consumption as accurate as possible.

One of the main damage mechanisms affecting power plant components is creep damage. Creep is the progressive plastic deformation of the metal under a constant load at high temperature, which ultimately leads to fracture when the component can no longer stand the load. The high temperature is relative term that depends on material. For power plant steels the creep takes place at the temperatures of 400 °C and higher (Table 1.1). The metal creep results in increasing of the linear size of the component and in thinning of the wall. The failure of the component happens at the deformation that is much less than deformation determined in the short-term tension test of the metal.

Table 1.1. Temperature of transition from low-temperature region to creep range [1].

Steel	Temperature
Non-alloyed steels	400 °C
Mn-alloyed steels	410 °C
17MnMoV6-4	420 °C
15NiCuMoNb5	420 °C
15Mo3	470 °C
13CrMo4-4	480 °C
10CrMo9-10	470 °C
14MoV6-3	500 °C
X20CrMV12-1	480 °C
15GS, 12Ch1MF, 15Ch1M1F	450 °C
12Ch18N12T	525 °C
12Ch11V2MF (EI-756)	550 °C

In order to determine the creep strength of the material the creep test is used [2, 3]. In a creep test a constant load is applied to a tensile specimen maintained at a constant temperature. Strain is then measured over a period of time. The tests are performed for a periods of time from 1,000 hours to 10,000 hours. The form of a

typical creep curve of strain versus time is shown in Figure 1.1. The slope of the curve is the strain rate of the test or the creep rate of the material. The creep curve may be divided into three stages. The first stage creep (primary creep) is characterised by a decreasing creep rate. The second stage creep (secondary creep) is characterised by relatively constant creep rate, which also represents the minimum rate. The third stage creep (tertiary creep) corresponds to an increasing creep rate, which ends in the rupture of the specimen. Creep strength is a stress, which causes a definite creep strain after a specified period of time at a given
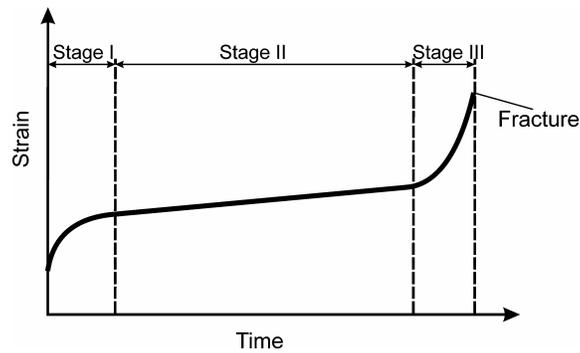
Figure 1.1. Creep curve of strain versus time during creep under constant load and three stages of creep

temperature. Creep strength of a material is much lower, than its tensile strength.

In addition to determination of the relation between deformation and time it is also important to know the total amount of deformation at the elevated temperatures, which the material can experience before it, ruptures. For that goal the creep rupture test is used [2, 4]. Creep rupture testing is similar to creep testing except that the stresses used are higher than in a creep test. Higher stresses are applied in order to obtain rupture of specimen in reasonable time (100 to 5,000 hours). So, creep rupture testing is always done until failure of the material. The main goal is to determine the creep rupture strength – a stress, which causes a fracture of a metal after a specified period of time at a given temperature. The stress is generally plotted against the time to rupture at a constant temperature on log-log coordinates as illustrated in Figure 1.2.
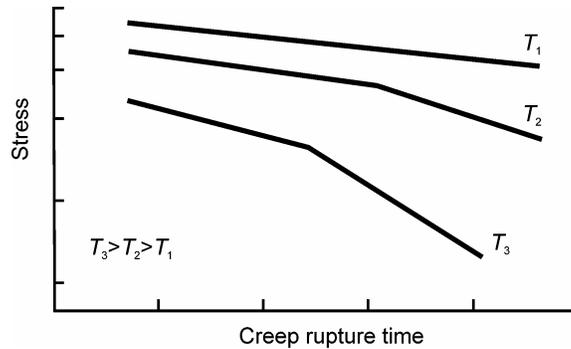
14

Figure 1.2. Creep rupture curves

The reliable data of the metal creep behaviour can be obtained only from the tests performed at service temperatures and stresses which occur in the real conditions of operation. Under these circumstances, however, the tests take a very long time. Therefore, the practical alternative is to carry out accelerated creep or creep rupture tests at higher temperatures or stresses in order to reduce the duration of the tests. The tests data can then be extrapolated to the time-temperature-stress regime of interest using parametric relationships [5, 6]. Larson-Miller parameter is one of the most well-known of these parametric relationships which relates the stress and temperature to the time to failure or specified creep strain. Use of the Larson-Miller parameter is based on the observation that creep is a thermally activated process and that the creep rate can be described by an Arrhenius-type expression of the following form

$$\frac{1}{\tau} = A \cdot e^{-\frac{Q}{RT}}. \tag{1.1}$$

After rearranging and multiplying by T, Eq. 1.1 becomes

$$\frac{Q}{R} = T\left(C + \log \tau\right) \tag{1.2}$$

or

$$P_{LM} = T\left(C + \log \tau\right), \tag{1.3}$$

where the constant C related to the constant A in Eq. 1.1. For perlitic and austenitic steels the constant C varies in the range of 18–22, for ferritic and ferritic-martensitic steels 24–25 [7]. The results of creep or creep rupture tests are often presented in terms of graph, where Larson-Miller parameter is plotted against the stress obtaining a master curve of the creep rupture behaviour.

It is well-known, that long-term operation of the metal in the conditions of creep causes the degradation of the metal structure [8, 9]. During operation at high

temperatures the precipitation and coarsening of carbides takes place due to transition of alloy elements into carbide phase. At the same time the quantity of carbides decreases. That fact explains the deterioration of mechanical properties of pearlitic steels since carbides serve as obstacles to dislocation movement and hence inhibit plastic deformation or creep. The kinetics of carbides precipitation and coarsening process and as well as content of alloy elements in carbides depend on temperature, stresses and service time and could serve as a criterion for evaluation of the metal condition. The spheroidization of cementite also occurs during service time in creep range. The spheroidization increases considerably the rate of creep whereas the decrease of tensile strength of the steel due to spheroidization is insignificant (10–15% [7]).

Long-term operation in conditions of creep is related to the appearance of cavities on the grain boundaries. Then these cavities gradually form chains, then microcracks by linkage and macrocracks which initiate rupture. Classification of structure damage based on distribution of creep cavities is presented in Figure 1.3. On the basis of accumulated damage of metal structure the life consumption of metal could be roughly estimated [10] (also presented in Figure 1.3). Structure damage parameters for steels manufactured in accordance with EN 10028 (*e.g.* 13CrMo4-4, 10CrMo9-10, X20CrMoV12-1 *etc.*) are presented in [11, 12].
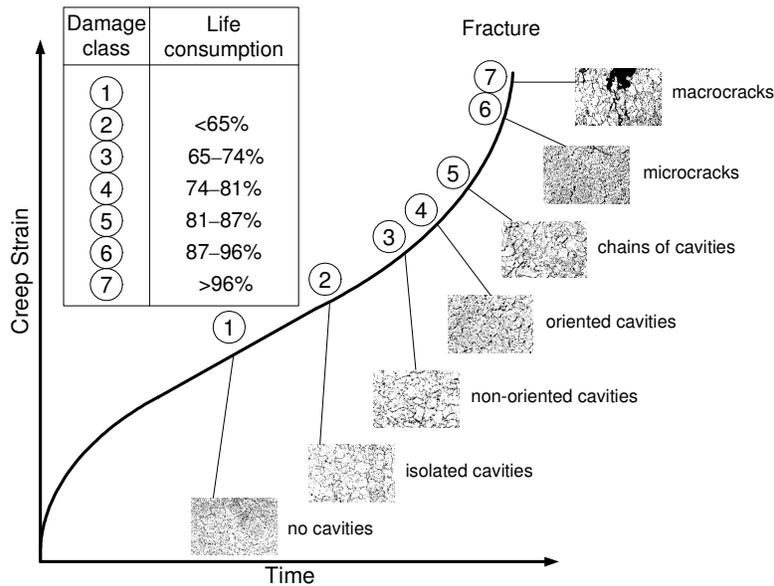

Figure 1.3. Scale of metal structure accumulated damage and life consumption depending on damage class

Thus the changes in metal structure reflect in some extent the ageing of material operated at high temperature and hence analysis of microstructure provides

important information in order to assess the creep damage degree of the metal. The microstructural analysis can be performed by means of *in situ* metallography, replication or sample extraction. It should be mentioned, that metal structure analysis by means of metallographic sample investigation has considerable advantage in comparison with method of replica because it is more representative and adequate and in complicated cases provides opportunity to perform analysis repeatedly. In addition, the creep cavities (voids) could become apparent or be developed during repeated polishing and etching [13].

As it was described above, long-term operation at high temperatures leads to altering in microstructure of metal. On the other hand the metal structure degradation can cause the deterioration of metal short-term mechanical properties determined at room temperature that decreases the durability of power equipment components. Therefore, evaluation of mechanical properties of metal of power plant components is highly significant in order to make reliable assessment of the material degradation degree. The mechanical properties of the metal are often taken from the tests of new material or conservative lower-bound curves published in design codes, which do not correspond to the properties of the particular material of the examined component due to experimental scatter, need of extrapolation to longer duration and changing of properties during operation. That leads to a large uncertainty in the evaluation of the state of metal damage. Thus in order to get reliable results the metal of the actual component in-service should be tested.

The degradation of the metal is often assessed on the basis of long-term mechanical properties [14]. However, paradoxical results of creep rupture tests of the metal operated at high temperature during the long period of time are presented in [7]. After creep rupture tests of large-scale specimens (with diameter of 10–15 mm) of the steel 12Ch1MF have been performed the specimens with diameter of 5 mm fabricated from two halves of the fractured specimens have been subjected to the same tests. The results have shown that creep rupture strength of the previously tested specimens decreased insignificantly whereas the total elongation did not change. In another series of experiments the tubular specimens of steel 12Ch1MF under internal pressure have been tested. From the undamaged parts of the ruptured tubes after the creep rupture testing the cylindrical specimens have been fabricated and tested. The results have shown that the stress rupture strength of the tubular specimens extrapolated to 100 thousands hours was about $62\,\text{N/mm}^2$, whereas for cylindrical specimens the creep rupture strength was even higher, namely $73\,\text{N/mm}^2$. The similar results are presented in [15], where it is shown that the greatest change in the long-term strength of the tubes was found to be in the initial period of service (in the course of 50,000 to 100,000 h), after which stabilization took place. It means that at least in the course of 200,000 hours of operation creep rupture strength of the service exposed metal approximates to the rupture strength of new material (Figure 1.4). In author's opinion [7] the assessment of steam piping integrity only on the basis of the results of long-term tests of the service exposed metal could result in wrong conclusions.
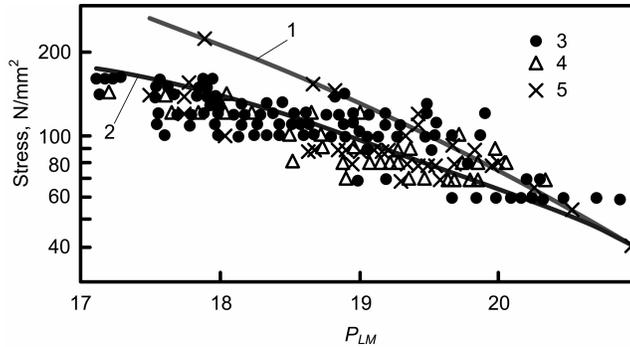
Figure 1.4. Results of the creep rupture tests of the steel 12Ch1MF after operation within 50–200 thousands hours (1 – new material, 2 – after various periods of service time, 3 – after 50–100, 4 – after 100–150, 5 – after 150–200 thousands hours of operation

The degradation of short-term mechanical properties is also observed during long-term operation in the conditions of creep [7, 16–21]. The influence of long-term operation on mechanical properties of perlitic steel 12Ch1MF, which is commonly used in steam piping manufacturing, was investigated in [7]. The results have shown that an exposure of steel 12Ch1MF to elevated temperatures leads to decreasing of tensile strength measured at room temperature. Tensile strength, measured at operating temperature, decreases more markedly, however, the correlations between tensile strength degradation and service time are not presented due to high scatter of test results. Moreover, author proposes to use the ratio of tensile strength measured at operating temperature to tensile strength measured at room temperature as one of reliability parameters since this ratio also steadily decreases during operation and has much less scatter. According to [7] the minimum allowable value of the ratio for steel 12Ch1MF is 0.48 at 560–570 °C and 0.55 at 540–545 °C.

The influence of long-term operation at high temperatures on yield strength measured at room temperature of steels 12Ch1MF and 2¼Cr-1Mo [16–19] is presented in Figure 1.5. Steel 2¼Cr-1Mo, which is also used for manufacturing of steam piping and headers, has been investigated in [20]. The results of investigation have shown an evident tendency of the subsequent yield strength decrease during service time. It is seen, that after 200 thousands hours of operation at 540 °C yield strength of steel 12Ch1MF decreases approximately by 7%, and for steel 2¼Cr-1Mo the decrease of yield strength is 24%. Investigation of a steel Cr-Mo-V for turbine rotor [21] has shown the decrease of tensile strength and yield strength after 200 thousands hours of operation at 530 °C from 939 N/mm^2 to 855 N/mm^2 (9%) and from 786 N/mm^2 to 686 N/mm^2 (13%) respectively. According to investigation of carbon steel 20 [22], operation at 450 °C leads to decrease of

tensile strength by 13% and yield strength by 20% after 79 thousands hours of operation. Consequently, long-term exposure at elevated temperatures in the conditions of creep results in a degradation of the short-time mechanical properties of metal for all investigated power plant steels.
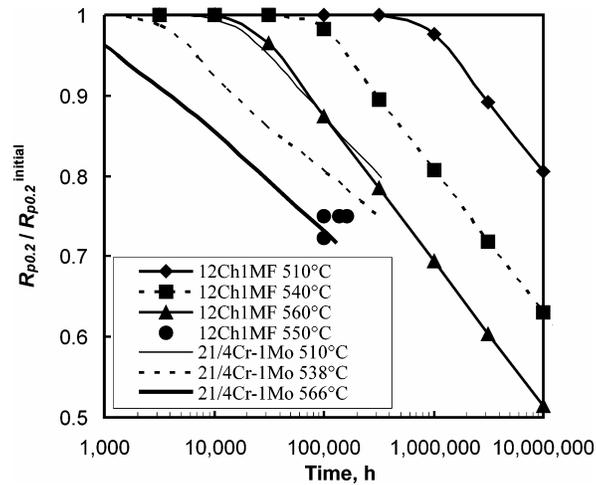
Figure 1.5. Effect of service time and temperature on the yield strength of steels 12Ch1MF [18, 19] and 2¼Cr-1Mo [20]

On the basis of investigation of mechanical properties deterioration kinetics the decrease of short-time mechanical properties for some power plant steels is specified in standards [23]. So, the decrease of short-time mechanical properties (tensile strength and yield strength) after 100 thousands hours of exposure for metal of pipeline straight sections and bends, which are operated in conditions of creep, more than 30 N/mm^2 compare with requirements for the new material is forbidden. Measured at temperature of 20 °C yield strength of metal of steam turbine casing should not be less than 255 N/mm^2 for steel 15Ch1M1FL and 245 N/mm^2 for steel 20ChMFL. The ratio of yield strength to tensile strength measured at room temperature ($R_{p0.2}/R_m$) should also satisfy certain requirements (*e.g.* for metal of feed water piping the ratio should not exceed 0.65 for non-alloyed steels and 0.75 for alloyed steels [23]).

Thus, the decrease of short-term mechanical properties determined at the temperature of 20 °C could be reliable factor of the creep damage evaluation in addition to analysing of metal structure.

19

2. DETERMINATION OF MECHANICAL PROPERTIES OF THE METAL OF IN-SERVICE COMPONENTS

2.1. Indirect techniques of the mechanical properties determination

Traditional destructive methods of mechanical properties evaluation by means of tension tests of standard specimens require removing metal from the component in great quantities and hence the replacement of the component. Therefore in order to reduce the cost of the metal examination and to determine the material properties of the in-service components without necessity of the replacement indirect techniques of the mechanical properties evaluation have been developed. These techniques are based on the relationship between tensile properties and hardness, which can be measured without metal removing by using of portable hardness testers. In this case prior to hardness testing it is necessary just to polish the surface of the component. Particularly, for determining the tensile strength and yield strength of some Russian steels, which are used for manufacturing of the basic components of power plants in Estonia, are used methods of SMiS "Donbassenergo" and Ural VTI [24, 25]. The equations of Brinell hardness number (HB) conversion into tensile properties of some steels are presented in Table 2.1.

Table 2.1. Relationship between tensile properties and Brinell hardness [24, 25]

Technique	Tensile properties (R_m, $R_{p0.2}$), 10^{-1} N/mm^2	
	12Ch1MF	15Ch1M1FL
SMiS "Donbassenergo"	HB=100–175 $R_{p0.2}$=0.545 HB-48.0	HB=130–160 $R_{p0.2}$=(0.33 HB-12.2)/1.21 HB=160–200 $R_{p0.2}$=(0.33 HB-23.1)/0.87
	HB=100–175 R_m=0.35 HB HB≥175 R_m=0.36 HB	R_m=0.328 HB+2.0
Ural VTI	$R_{p0.2}$=0.235 HB+1.8	HB<200 $R_{p0.2}$=0.29 HB-11.4 HB>200 $R_{p0.2}$=0.57 HB-62.7
	R_m 0.335 HB+1.8	R_m=0.29 HB+8.0

In order to analyse the validity of using above-mentioned methods, the results of metal testing during many years in the laboratory, are taken into consideration. The values of tensile strength and yield strength obtained from the tension tests of standard cylindrical specimens and Brinell hardness measured by means of bench-top testers have been selected. Calculated and measured at temperature of 20 °C tensile properties of the steel 12Ch1MF depending on Brinell hardness are presented in Figure 2.1. It is seen, that the results of the real direct tensile tests and

calculated data have shown quite a good agreement. However the ratio of yield strength to tensile strength could not be practically predicted on the basis of hardness values with acceptable accuracy.

Figure 2.1. Relationship of tensile strength, yield strength and Brinell hardness of the steel 12Ch1MF. Measurements were conducted at temperature of 20 °C. The lines represent correlations according to methods of SMiS "Donbassenergo" and Ural VTI

The measurements conducted at operating temperature of 540 °C have shown significantly higher scatter of the data (Figure 2.2). Also it is impossible to find functional relation between yield/tensile ratio and service time (Figure 2.3) or between yield/tensile ratio and tensile strength at room temperature (Figure 2.4). Thus, it is valid to consider, that it is impossible to estimate the yield strength depending on measured tensile strength with acceptable accuracy. At the same
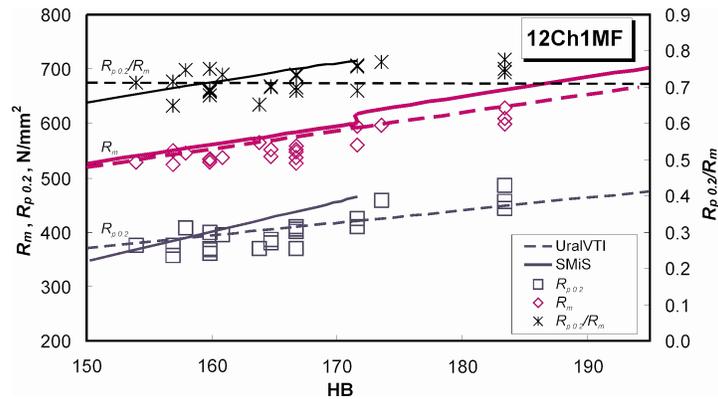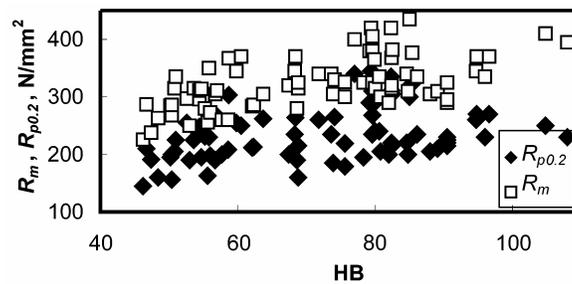

Figure 2.2. Relationship between tensile strength, yield strength and Brinell hardness of the steel 12Ch1MF. Measurements have been conducted at temperature of 540 °C

21

time the yield strength is a very essential parameter for the operational integrity assessment of some components (*e.g.* turbine casing).
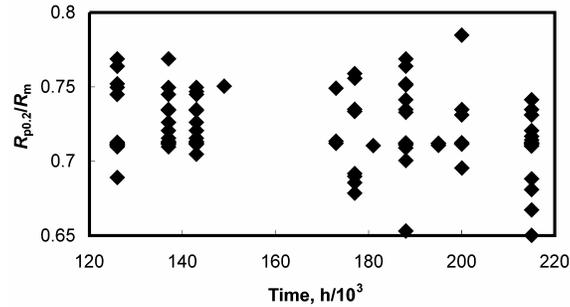
Figure 2.3. Relationship between the ratio of the yield strength to tensile strength of the steel 12Ch1MF and service time
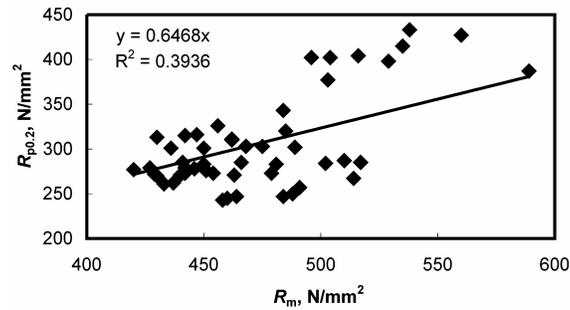
Figure 2.4. Relationship between the yield strength and tensile strength of the steel 12Ch1MF

   Another comparative analysis of real tensile properties and converted from hardness values has been carried out. Tensile properties have been determined by tensile testing of the miniature flat specimens (detailed description of the tests performance could be found in Chapter 2.3 of the present work), which have been fabricated from the samples extracted from the power equipment components. The metal hardness has been measured by portable testers (type 54-359 M) on the surface of the dimple, where samples have been extracted from. It should be mentioned, that the hardness has been measured not from the surface layer but at a depth of about 2–3 mm from the surface of the component, that represents the properties of bulk metal. The results of tensile testing of miniature specimens, conducted at room temperature, were compared with calculated values depending on metal hardness. In Figure 2.5 it is clearly seen, that the values, predicted by

correlations, are significantly higher, than the values of mechanical properties, obtained from direct tensile testing. Moreover a wide disagreement with proposed in [24, 25] relations is observed for both investigated steels (12Ch1MF and 15Ch1M1FL). The ratio of yield strength to tensile strength also practically could not be predicted.
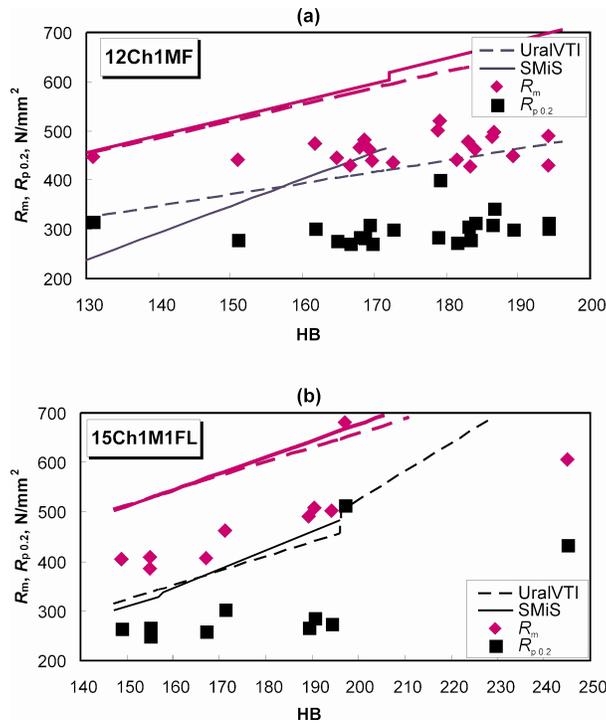
Figure 2.5. Relationship between tensile strength, yield strength and Brinell hardness of steels 12Ch1MF (a) and 15Ch1M1FL (b). Measurements were conducted at temperature of 20 °C. The lines represent correlations of SMiS "Donbassenergo" and Ural VTI

It should be briefly mentioned, that automated ball indentation (ABI) technique [26] could be also applied to evaluate the mechanical properties of metal. ABI is non-destructive technique, which is based on ball indentation and the uniqueness of which is the fact that this technique does not require post measurement of the diameter of indentation. According to [26] ABI allows determining several mechanical properties (*e.g.* yield strength, tensile strength). However, plasticity of the metal (percent elongation and reduction of area, which are very important

parameters in estimation of durability of such components as boiler drums, piping) could not be measured by this technique, neither by conversion of hardness values.

In addition, it should be emphasised, that in contrast to direct tensile tests neither ABI technique, nor the converted hardness values do not provide the information whether obtained tensile properties are in the longitudinal or transverse direction. It should be also pointed out, that both of the methods provide data about properties of the surface layer of the component, which are unrepresentative of bulk metal properties. So, in view of surface effects such as oxidation or carbon depletion, either during manufacturing or in service, mechanical properties of the surface layer are significantly different from properties of the bulk metal.

To sum up, the mentioned indirect techniques could not substitute the direct tensile tests and the tensile properties of the actual material can be obtained only by means of direct tensile testing. The complete material behaviour could be adequately and reliably depicted only by the entire stress-strain curve, which could not be provided by indirect techniques.

2.2. Sampling devices for metal extraction from power plant components

As it was considered in Chapter 1 in order to predict the degree of the metal degradation and integrity of the component the determination of the mechanical properties of the actual component in-service material is required. In order to estimate the mechanical properties the metal sample should be extracted from the actually exposed components since the only reliable and adequate method of the material properties determination is direct testing. Traditional methods of mechanical properties evaluation require large specimens (not less than 20 mm in length) and cannot be applied since it is impossible to obtain such a quantity of metal from a component in service without degrading its integrity. Therefore over the past two decades, a number of sampling techniques have been developed with aim of overcoming the problems associated with the removal of large amount of materials from the components under examination. A detailed review of metal sampling methods could be found in [27–30]. It should be only emphasised, that, in accordance with cutting principle, all these methods are divided into the following two basic types: the first is based on mechanical sample extraction and the second is electro-discharge machining.

In view of the very high cost and massiveness of the previously developed sampling machines it was decided to design sampling devices for metal extraction from external and internal surfaces of components that are more compact, portable, convenient and cheap.

Operation principle of designed devices is based on mechanical extraction. The cutting element is hemispherical shell saw with diameter of 60 mm and wall thickness of 0.4–0.5 mm. The cutting edge of the saw is coated with abrasive coating (natural diamond or CBN). The hemispherical saw rotates around its axis of symmetry and at the same time moves round the axis, which is normal to

rotation axis (and parallel to Y axis, Figure 2.6). The maximum thickness of the extracted sample is about 2.2 mm. The geometry and size of sample are formed as intersection of sampled area and sphere with diameter about 58.7 mm (Figure 2.7).
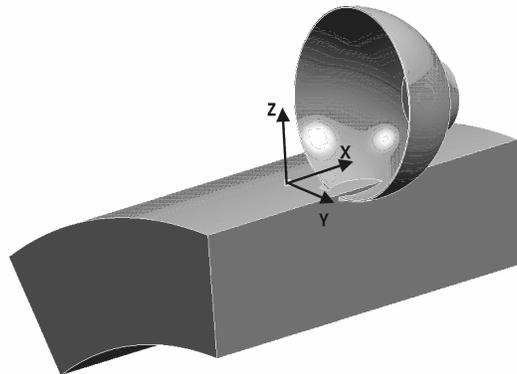
Figure 2.6. Principle scheme of sample extraction
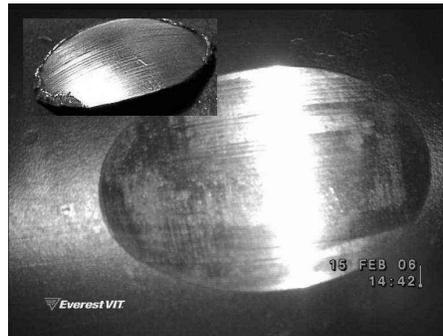
Figure 2.7. Metal sample and remained spherical dimple on the internal surface of the turbine K-200-130 high pressure rotor bore

The depth of the dimple after sample extraction could be up to 3.0 mm, that is defined by the quality (thickness) of abrasive coating of the cutting bit and quality of the hemispherical shell saw manufacturing. The latter is important to guarantee the success of extraction process. Poor quality of the saw could cause jamming and emergency outage of cutting tool before the extracting process is completed. If the sampling is performed from the external surface of the component where the access to sampled area is generally easy, the uncompleted extraction leads only to the loss

of the sample. In this case the area of unsuccessful sample extraction could be simply mechanically treated to minimise stress concentration. As regards the case of uncompleted extraction of the sample from internal surface of turbine rotors bores, removing of the formed stress concentrator is a rather difficult process, which is similar to the process of sample extraction itself. Therefore high quality of the cutting tool manufacturing is required.

During sample extraction the area in the vicinity of cutting is cooled by solution of water and concentrate of standard emulsion for mechanical cutting in the ratio according to recommendations of emulsion producers.

Tallinn University of Technology (TUT) has experience of metal sampling of miniature specimens from Estonian power plants equipment components (basically at Narva Power Plants) since 1997. An overview of this experience and description of designed and manufactured sampling devices for metal extraction from external and internal surfaces of controlled power plant components are presented in the following chapters. More detailed description of experience in metal sampling is presented in [III].

2.2.1. Sampling machine for extraction from external surface of the component

Sampling device for metal extraction from external surface of the components (MSM-1) is presented in Figure 2.8. The hemispherical shell saw is rotated by electromechanical drive. MSM-1 is additionally equipped with controller of speed of rotation of the saw.

The system of electromechanical drive with a cutting tool is mounted on the working frame that provides moving of the saw around its own axis, which is parallel to Y axis (Figure 2.6) and normal to rotation axis of the saw. The distance between working frame and sampled area is adjusted by means of four screws, located in the corners of the frame. This distance and the shape of the surface of the sampled area define the thickness of the sample. Four magnet holders, which hold sampling device on the component, are hinged to the screws. Every magnet holder consists of three constant magnets and stippler in the centre, which prevents sampling device from moving on the surface of the component.

The system of feeding consists of stepping-motor and gear sector on which cutting tool is firmly fixed. The speed of stepping-motor rotation, which defines the speed of feeding, is remotely controlled through the microstepping driver (IM483I). The program of cutting parameters is saved in NVM (non-volatile memory) of microstepping driver. Moreover, such system allows remote controlling of cutting process in online regime (through RS232 interface), and tracking the location of cutting tool (if an encoder is present). Theoretically the speed of cutting/feeding could be variable during metal sampling: at the initial and final stages the speed could be higher, than in the middle of sampling process, because the contact area between cutting tool and surface of the component is variable during extraction. Therefore, for the intensification of the cutting process

the speed of feeding could be changed, depending on the position of cutting tool. However, the program of constant feeding speed, which is optimal for maximum area of contact surface, is realised in presented sampling device because the effect of changing the feeding speed is small (relating to total consumption for sampling and initiation of additional risks).

Figure 2.8. Device MSM-1 for sampling from external surface of power plant components

The speed of rotation of hemispherical shell saw of presented device is about 8,000 rpm. According to experience of Thermal Engineering Department of TUT, the optimal duration of extraction of one sample (leaving out of account the time of adjustment and setting of the device) is about 45 minutes. Totally more than 200 samples have been extracted from external surface of steam pipes, turbine casings, and drums by means of this device since sampling device was designed.

2.2.2. Sampling machine for extraction from internal surface of the component

Sampling device for metal extraction from internal surface of turbine rotors bores (MSM-2) is presented in Figure 2.9. Cutting tool of this device is driven by air turbine through flexible shaft. The speed of rotation of hemispherical shell saw is about 10,000–15,000 rpm.

Feeding system is also based on using of stepping-motor and microstepping driver (IM483I). The systems of driving, feeding and auxiliary systems are located
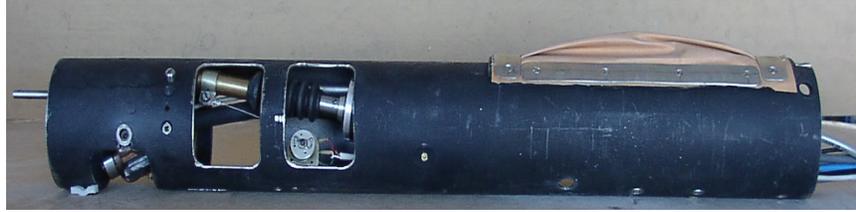
Figure 2.9. Sampling device (MSM-2) for sampling from bores

inside the tube of 88 mm in diameter (outside) and 620 mm in length. This tube is hinged with another auxiliary tube of less diameter and 1600 mm in length, which serves as a holder of sampling device. All cables and hoses are placed inside this auxiliary tube. The total length of both tubes allows extract samples at the significant distance from the end of the bore. Prior to extraction sampling device is fixed inside the bore in two sections, which are normal to the axis of the device. In the first section, near the cutting area (front edge of the device), fixation is realised by means of two rods, which are equidistant (45 degrees) from the vertical plane, passing through the tube axis and lower support point of the device. In inoperative position these rods are hided inside the device frame and for the fixation of the device they are pulled out by the drive of pneumatic cylinders. Rear of the device is fixated by air bag. The thickness of the metal sample could be also adjusted and the maximum thickness is about 1.9 mm. The minimum diameter of sampled bore is 95 mm.

Extraction without direct eye contact requires beside high quality of cutting tool some extra equipment to control the sampling process. Therefore, the device MSM-2 is additionally equipped by auxiliary systems. One of them is the system of rotational speed measurement and indication, on the basis of which the current state of extraction process could be estimated. Thus, in case of need the feeding could be temporally stopped that could prevent the cutting tool from jamming. Moreover sampling device is equipped by cutting tool position sensor and limit stop, which turns on the saw reverse to the initial position. Cutting process could be also remotely controlled in online regime as well as in case of MSM-1. Duration of one sample extraction is about 90 minutes.

Design and technical composition of MSM-2 as well as control panel are protected by Estonian utility models certificates [31, 32].

2.2.3. Stress distribution in the power plant components after sampling

The metal sampling from the in-service components can be performed only when the sample size is so small that remained dimple on the surface of the component does not cause the inadmissible increase of stresses and does not require the sampled area to be repaired. In other words the sampling should be minimally invasive and allow continued exposure without degrading of integrity of the

component. On the other hand, the sample should be big enough for mechanical properties determination. However, if there are any doubts about the remaining life and the possible failure of the component due to sampling, above mentioned techniques of small samples removing could not be applied. Therefore, in order to analyse the applicability of the sampling from the in-service components the impact of the dimple to stress distribution in pipes and turbine rotor has been analysed applying finite elements (FE) method. The commercially available packet ANSYS has been used for that goal [53].

3-dimensional model of turbine rotor has been used to analyse the affect of sampling on the stress concentration in the dimple. The size of the dimple has been chosen corresponding to the size of the real dimple in the rotor bore with 3 mm in depth. The turbine rotor model has been loaded only with centrifugal force due to rotation at 3000 rpm. The stress distribution in turbine K-200-130 rotor in the vicinity of dimple is presented in Figure 2.10. As it could be seen the maximal stress is located on the bottom of the dimple.
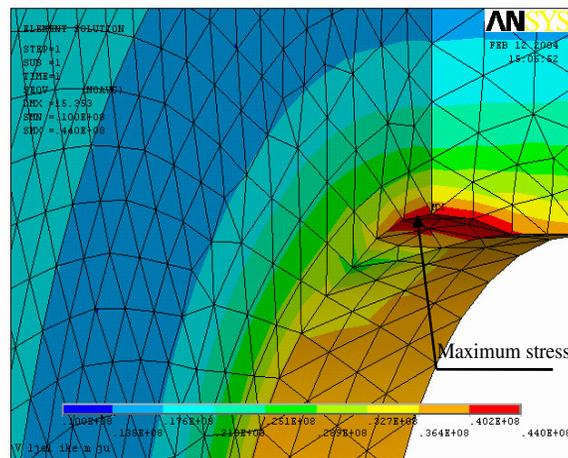
Figure 2.10. 3D stress distribution in turbine rotor in the
vicinity of dimple

On the basis of the results the stress concentration factors has been calculated as the ratio of the maximal stress in the bottom of the dimple to the stress the internal surface of the undamaged rotor. The results have shown that stress concentration factors on the bottom of dimple for turbine rotors with different sizes equal to 1.2 and 1.19 where the less value corresponds to the more massive rotors.

It should be mentioned that the hypothesis that two diametrically located dimples on the surface of rotor bore decrease the stress concentration has been also examined. The stress concentration factors for both dimples equal to approximately

1.28 and hence removing of two samples from two diametrical locations of the rotor bore do not decrease the stress concentration.

The impact of sampling on the stress distribution in pipe wall has been analysed by means of model of straight pipe under internal pressure. The depth of the dimple has been in the range 1–4 mm. The stress distribution in the vicinity of dimple on the external surface of pipe is similar to the case of turbine rotor. The maximum stress is located on the bottom of the dimple. The stress near the edge of dimple is significantly smaller, Figure 2.11. The stress distribution along wall thickness for different depth of dimple is presented in Figure 2.12.

Figure 2.11. Stress distribution in pipe wall after sampling

Figure 2.12. Stress distribution in pipe wall depending on the depth of the dimple

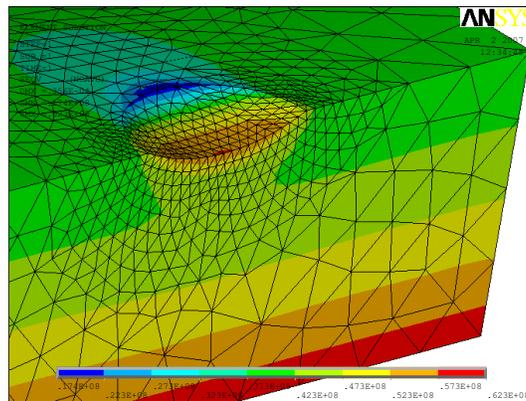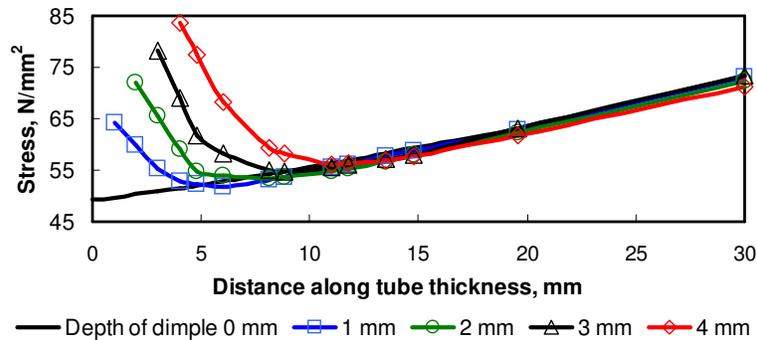The deeper is the dimple the greater is the maximum stress on the bottom of the dimple. In the case of small depths of dimple (1 mm and 2 mm) stress on the bottom of the dimple does not exceed the stress on the internal surface of undamaged pipe.

The stress concentration factor calculated as ratio of the stress on the bottom of dimple to the stress on undamaged pipe wall in the same depth from pipe external surface is shown in Figure 2.13.
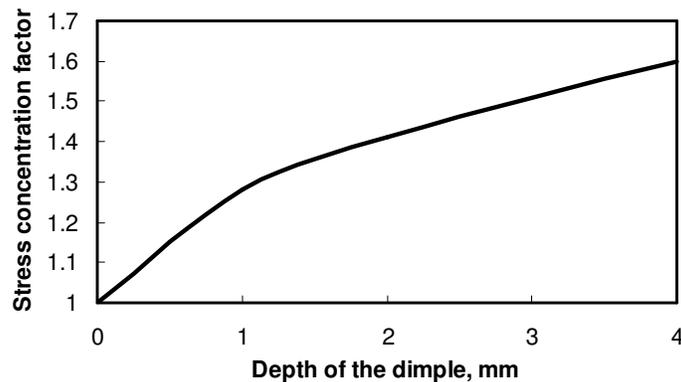
Figure 2.13. Stress concentration depending on the depth of the dimple
for a pipe Ø325×30 mm

In practice the depth of the dimple does not exceed 3 mm. The impact of dimple with this depth on the stress concentration in pipes with various diameter, wall thickness and internal pressure (14 MPa and 2.3 MPa) has been analysed. The greatest wall thickness corresponds to the TP-67 type boiler drum. The results have shown that the stress concentration factor for pipe wall thickness greater than 30 mm is approximately 1.5. Decrease of the pipe wall thickness leads to increase of the stress concentration factor, (see Figure 2.14).

Modelling of sampling with saw diameter of 50 mm has been also performed. The results have revealed that smaller diameter of the cutting hemisphere causes higher stress concentration but in most cases maximal stresses in dimples do not exceed allowable stress value.

Drawing the conclusions from the FE analysis of the stress distribution in the vicinity of the dimple of the power plant components after sampling the following results should be emphasised. The stress concentration factor on the bottom of the dimple on the surface of turbine rotor bore is approximately 1.2. Two diametrically located dimples on the surface of rotor bore do not decrease the stress concentration on the bottom of these dimples. The stress concentration factor on the bottom of the dimple on the external surface of pipe depends on the depth of the dimple and on pipe wall thickness. The stress concentration factor for dimples of 3 mm in depth does not exceed 1.5.
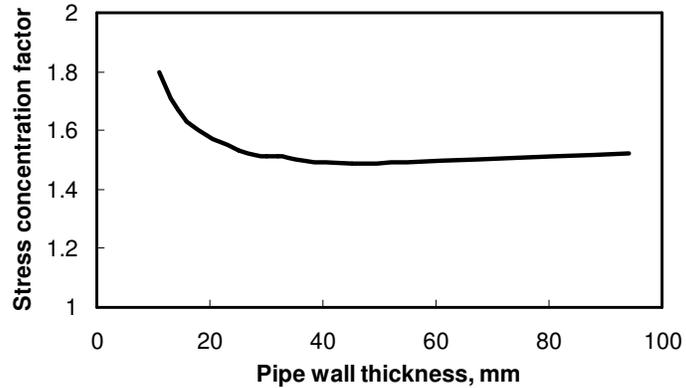
Figure 2.14. Stress concentration depending on pipe wall thickness for
dimple of 3 mm in depth

Thus, the method of small samples extraction does not lead to initiation of inadmissible stress concentrations and in the most cases maximal stresses in dimples do not exceed allowable stress values. It means that metal sampling by means of designed sampling machines (MSM-1 – for sampling from external surface of pipes, boiler drums and turbine casings and MSM-2 – for sampling from internal surface of turbine rotor bore) could be used without sacrificing of the safety of the in-service components and does not require the sampled area to be repaired. The designed sampling devices have been successfully implemented in power plants of Estonia. Totally more than 200 samples from external surface of steam pipes, turbine casings, drums and internal surface of turbine rotors have been extracted so far.

2.3. Small punch testing

2.3.1. Introduction

Since the metal samples extracted from in-service components should be small enough in order to allow continued safe operation, the problem of tensile properties obtaining from the limited amount of metal has arisen. Over the past two decades a number of miniaturised specimens testing techniques have been developed. One of such techniques is small punch (SP) testing proposed by Manahan *et al.* [33]. This technique has attracted attention and has been investigated by many researchers [34–41]. In respect of evaluation of creep properties or fracture behaviour of the material the SP testing technique has been also investigated [42–50].

The SP testing technique is based on the determination of the curve of force versus displacement for a small disk-shaped specimen when a central force is applied. A typical SP force-displacement curve is presented in Figure. 2.15. A curve can be divided into four distinct regimes: I elastic bending, II plastic bending, III membrane stretching, IV plastic instability. The deformation mechanisms associated to different regimes have been studied in [51]. On the basis of SP test results the force corresponded to the limit of elastic regime and initialization of plastic deformation (P_y) and maximum force (P_{max}) can be determined. The relationships between these SP test parameters and tensile properties have been obtained and presented in [34, 36, 38]. It was found that tensile strength of the material is linearly related to maximum punch force. In evaluation of yield strength, however, there are two different approaches. Whereas in [36] the yield strength and maximum punch force have been shown to follow a linear law, in accordance with [34, 38] the yield strength of metal is linearly
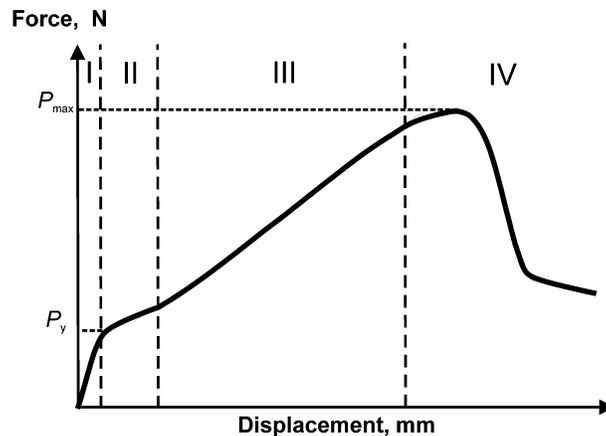

Figure 2.15. A typical small punch force-displacement curve

related to the limit of elastic regime in SP test. It should be mentioned that yield strength is very important parameter for estimation of metal condition (the allowable decrease of yield strength for some power plant steels is specified in [23]).

Despite a number of researches and reported FE studies of SP testing, this method is not yet standardised since the behaviour of the specimen in SP test is still not fully understood and any ideas to improve, develop and make the tests more reliable are very welcome. Standardization procedures for determining mechanical properties based on SP testing are being developed through cooperation by several laboratories using both experiments and mathematical models. Thus one of the objectives of the present work was to analyse the applicability of the determination of tensile properties of the power plant components material by means of SP testing technique.

2.3.2. Experimental

In order to analyse the applicability of SP testing technique for the determination of tensile strength and yield strength of some power plant steels SP tests and conventional tensile tests have been performed. The chemical composition of these steels is presented in Table 2.1. After extracting of 10 metal samples from steam pipes, superheater tubes (20, 12Ch1MF, 12Ch11V2MF) and drum (16GNM) components, 32 specimens for punch testing and 24 specimens for tensile tests have been prepared from these samples.

Manufacturing of standard cylindrical specimens and tension tests have been carried out in accordance with EN 10002-1:1996. The miniature disk-shaped specimens have been prepared with dimensions of 8 mm in diameter and 0.5 mm in thickness. The tests have been conducted on a testing machine Instron 8516 under a constant displacement rate of 2.5 mm/min. The SP test fixture is shown schematically in Figure 2.16. The specimen holder, consisting of upper and lower dies, supports the specimen. A thread on the dies, not shown in the scheme, is used to apply a clamping force. Thus a specimen disk is clamped between two dies to the width of 1 mm at the periphery by force of 7 kN. The specimen is subjected to a central force, which is transmitted from the punch to the specimen by means of a hardened steel ball 4.8 mm in diameter.

Table 2.1. Chemical composition of investigated steels

Steel Grade	Content, wt.%												
	C	Si	Mn	Cr	Ni	Mo	V	W	Nb	Ti	Cu	S	P
20[1,2]	0.17–0.24	0.17–0.37	0.35–0.65	max 0.25	max 0.3						max 0.3	max 0.04	max 0.035
12Ch1MF[1,2]	0.08–0.15	0.17–0.37	0.4–0.7	0.9–1.2	max 0.3	0.25–0.35	0.15–0.3	max 0.2			max 0.2	max 0.025	max 0.03
16GNM[1]	0.12–0.18	0.17–0.37	0.8–1.1	max 0.3	1.0–1.3	0.4–0.55					0.15–0.25	max 0.04	max 0.035
12Ch11V2MF[1]	0.10–0.17	max 0.5	0.5–0.8	11–13	max 0.6	0.6–0.9	0.15–0.3	1.7–2.2			max 0.3	max 0.025	max 0.03
X10CrMoVNb9-1[2]	0.08–0.12	0.20–0.50	0.3–0.6	8.0–9.5	max 0.4	0.85–1.05	0.18–0.25	-	0.06–0.1	-	max 0.3	max 0.04	max 0.035
12Ch18N12T[2,3]	max 0.12	max 0.8	1.0–2.0	17.9–19.0	11.0–13.0	-	-	-	-	max 0.7	max 0.3	max 0.02	max 0.035
X8CrNiNb16-13[3]	0.04	0.30–0.60	1.50	15.0–17.0	12.0–14.0	-	-	-	1.2	-	-	max 0.015	max 0.035
X8CrNiMoNb16-16[3]	0.04–0.10	0.30–0.60	1.50	15.5–17.5	15.5–17.5	1.60–2.00	-	-	1.2	-	-	max 0.015	max 0.035
B-407[3]	0.05–0.10	1.0	1.50	21.0	31.4	-	-	-	-	0.50	-	max 0.015	-

[1] – has been subjected to small punch testing;
[2] – has been subjected to tensile testing using miniature specimens;
[3] – has been subjected to corrosion testing.
    Grades of Russian steels are designated in accordance with [52].
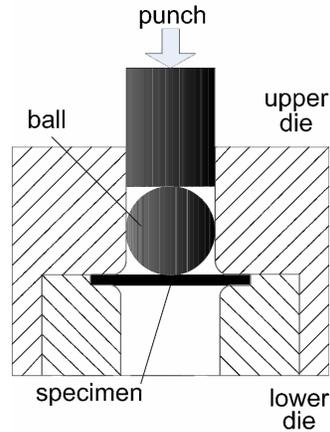
Figure 2.16. Small punch
testing fixture

2.3.3. Finite element modelling

A finite element model has been developed to calculate the force–displacement curve obtained from the SP experiment. The commercially available packet ANSYS has been used for that goal. Axissymmetrical elements (PLANE82) and (PLANE2) have been used for the specimen and punch ball, respectively. Surface-to-surface target element (TARGE169) and the contact element (CONTA172) have been employed to simulate the contact between the specimen and punch ball. A coefficient of friction at the specimen-ball interfaces of μ=0.3 has been assumed. The 2D finite element model (FEM) is presented in Figure 2.17. All nodes on the left side (along the axis of symmetry) have been constrained from moving in lateral direction. All degrees of freedom of the nodes where the specimen is clamped between the upper and down dies have been restricted.

The specimen and punch ball have been modelled with the following properties: Young's modulus E=2×10^5 N/mm^2, Poisson's ratio ν=0.3. The elastoplastic behaviour of the specimen material has been modelled using the multilinear isotropic hardening law. According to ANSYS requirements [53] the material law has been input in terms of true stresses and true strains. The upper portion of strain-hardening curve has been extrapolated from experimentally obtained necking behaviour in uniaxial tensile tests: R_m=443 N/mm^2 and R_e=300 N/mm^2.

A FE analysis has been performed for punch displacements imposed in the range of 0.0 mm to 2.2 mm. The resulting punch force has been obtained by summing the forces on the upper nodes of the ball.

36
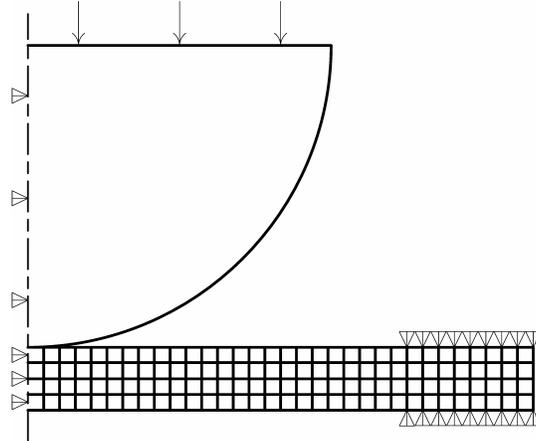
Figure 2.17. 2D finite element model of small punch
test

The FE model has also been used to determine the relationships between the specimen tensile strength and yield strength and the maximum punch force obtained from SP test. Two series of FE analyses have been performed for six different sets of material properties. In the first series three FE models have been created for the materials with the same tensile strength and different values of proportionality limit (Table 2.2). In the second series the materials with the same proportionality limit and different values of tensile strength have been used.

Table 2.2. Input properties of material for FE analysis

Property	First series			Second series		
Proportionality limit R_e N/mm^2	300	300	300	260	300	340
Tensile strength R_m, N/mm^2	380	443	500	443	443	443

2.3.4. Results and discussion

The results of SP and conventional tensile tests are partially presented in Table 2.3. The high repeatability (0–2%) of results of tensile strength determined from tension tests are contrasted to the significant lower repeatability (0–5%) among maximum force measurements from SP tests. In order to obtain the relationship between SP maximum force and tensile strength a linear least squares regression of experimental data has been performed and the following regression equation has been obtained (Figure 2.18):

$$R_m = 0.184 \cdot P_{max} \pm 53 \text{ N/mm}^2 , \qquad (2.1)$$

where ±53 – standard error of the regression equation in N/mm^2.

The results of FE analysis are in a good agreement with experimental data and have also shown that the maximum punch force is linearly related to tensile strength (Figure 2.18).

Table 2.3 Results of small punch and tension tests

Steel	Small punch test			Tension test		
	P_{max}, mean, N	Number of specimens	Repeat-ability*, %	R_m, mean, N/mm^2	Number of specimens	Repeat-ability*, %
12Ch1MF	3132	4	3	534	3	1
12Ch1MF	2479	2	2	480	2	0
12Ch1MF	2764	3	0	474	2	1
12Ch1MF	2423	3	1	455	2	1
12Ch1MF	2667	4	0	443	3	2
16GNM	2863	3	4	555	2	1
16GNM	2915	3	5	553	2	0
16GNM	3224	3	3	541	2	0
12Ch11V2MF	3846	5	4	823	3	1
20	2807	2	3	468	3	0

* – repeatability is calculated by dividing the standard deviation by the mean
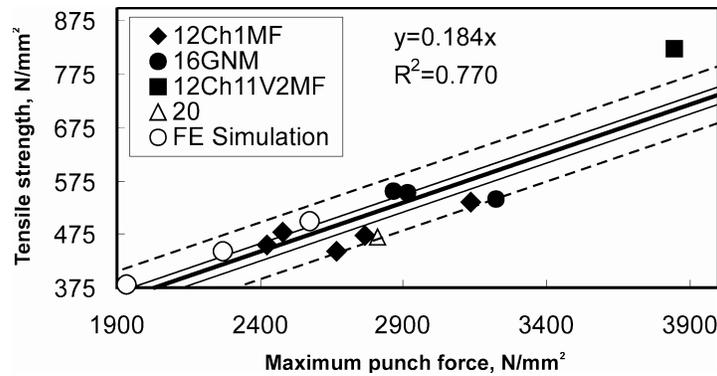
Figure 2.18. Relationship between SP maximum force and tensile strength of examined materials. Centre thick line represents regression equation (1), fine solid lines - standard error of the mean value, dash lines - standard error of the regression equation. Confidence probability is 68.3%

Figure 2.19 presents results from the FE modelling at a displacement of 1.0 mm and 2.2 mm. As it is apparent from the figure, a circumferential region can be observed where there is a considerable thinning of the specimen. These results are in a good agreement with the physical experiments, which have shown that the
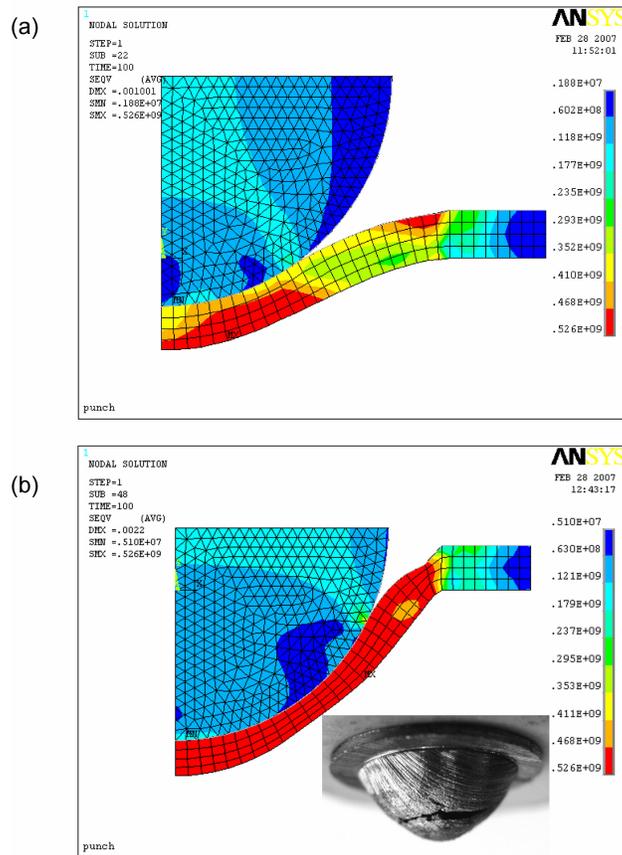
Figure 2.19. FE model of the SP testing at a punch ball displacement of 1.0 mm (a) and 2.2 mm with photo of tested specimen (b)

final failure of the specimen takes place exactly at this region (see photo in Figure 2.19 b). A comparison of force-displacement curves obtained from experiment and FE analysis is presented in Figure 2.20. Agreement in maximum punch force is quite good, location of FE maximum force along displacement coordinate depends on location of necking point at hardening curve used in FE model. The difference in displacement could be also explained by the test machine and punch compliance since the displacement of the punch tip is less

39

than the displacement of the machine crosshead which has been measured during experiments and taken into account in curve plotting.
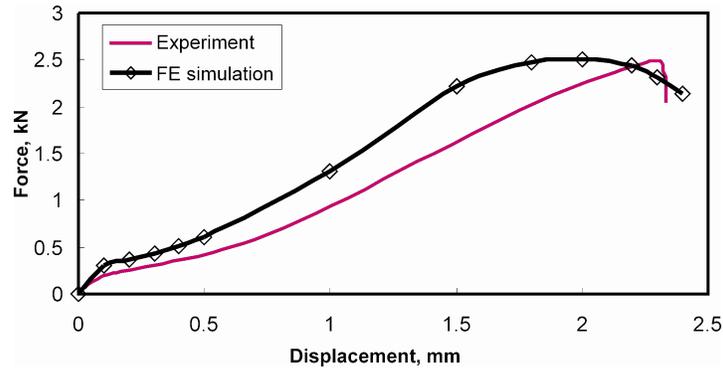
Figure 2.20. Experimental force-displacement curve compared with FE simulation

Yield strength determination from SP tests will now be considered in more detail. The relationship between the yield strength and maximum punch force has been investigated in [36] and shown to follow a linear law for an elastic-perfectly plastic material. However, if both characteristics, yield strength and tensile strength, are linearly related to the maximum punch force, then the ratio of yield to tensile should be constant. As it was outlined above (Chapter 2.1) there is no functional relationship between yield strength and tensile strength (Figure 2.4) and the ratio of yield strength to tensile strength varies in a wide range (Figure 2.3). This may be explained by the influence of such factors as creep embrittlement, corrosion embrittlement, etc.

The FE analysis of SP test has shown that the maximum punch force is the same for materials with different values of proportionality limit or yield strength (there is usually little difference between proportionality limit and yield strength) and with the same tensile strength (Figure 2.21 a). Moreover, different the maximum punch forces correspond to the materials with the same yield strength and different tensile strength (Figure 2.21 b). Thus the yield strength of post-exposed investigated steels cannot reliably be determined as a function of maximum punch force. Moreover, it is not clear how yield strength, which is determined by the force of transition from elastic region to plastic, could generally be estimated on the basis of the maximum punch force, which results from a plastically deformed, hardened material.
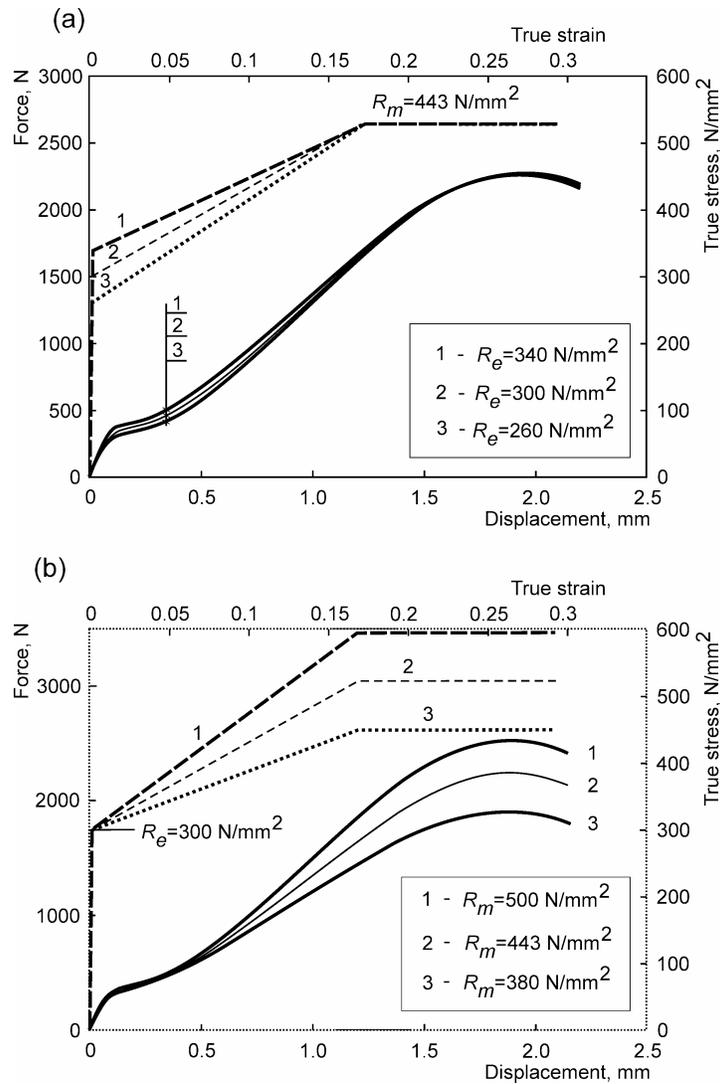
Figure 2.21. FE simulation of SP testing for materials with different proportionality limits (a) and tensile strength (b). Dashed lines represent the material law (true stress vs. true strain) as it has been input in ANSYS. Solid lines represent the FE simulation results (force vs. displacement)

So it could be concluded that the maximum punch force is not affected by the yield strength of the post-exposed investigated steels. According to another approach for yield strength determination from SP test proposed in [34, 38] the

yield strength can be determined as a function of force corresponded to the initialization of the plastic deformation. However, it has not appeared possible to determine the transition point from the elastic to the plastic region, from the SP force-displacement curves of the investigated steels (Figure 2.22). This means that the material yield strength could not be determined with sufficient accuracy using of SP tests, neither on the basis of maximum punch force nor on the basis of the force corresponded to the initiation of plastic deformation.
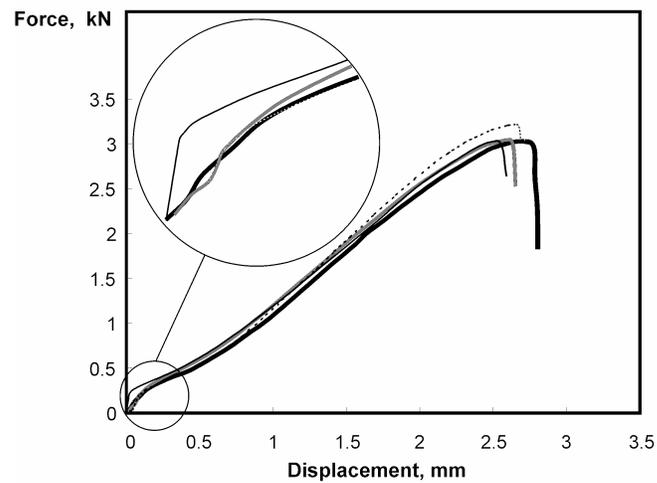
Figure 2.22. A force-displacement curve at room temperature obtained from SP tests of steel 12Ch1MF

42

2.4. Tension test of miniature specimens

In view of difficulties in determining of yield strength of the metal by means of small punch tests the decision to reject from this technique has been taken. Therefore the objective of present investigation was to develop the novel reliable technique of determination of mechanical properties of materials by means of tensile testing of miniature specimens and to compare the tests results with results of tension tests of conventional standard specimens.

2.4.1. Experimental

The tensile tests have been carried out using conventional cylindrical test specimens with standard size and miniature proportional flat specimens (with the gauge length defined as $L_0=5.65\sqrt{S_0}$, where S_0 is the cross area of the gauge section). The geometry of miniaturised tensile test specimen is presented in Figure 2.23 (all dimensions in mm). The thickness of the specimen is 0.5 mm. Thus according to European standards [54] the requirement, that the thickness of the specimen shell not be less than 0.1 mm, is in this case satisfied. The width of the gauge section of the specimen is 2 mm and hence the cross area equals to 1 mm^2. The gauge length is 5.65 mm and the total length of the specimen is 10.65 mm, that allows preparing 3–5 miniature tensile specimens from one sample extracted by means of sampling device designed in TUT [III].
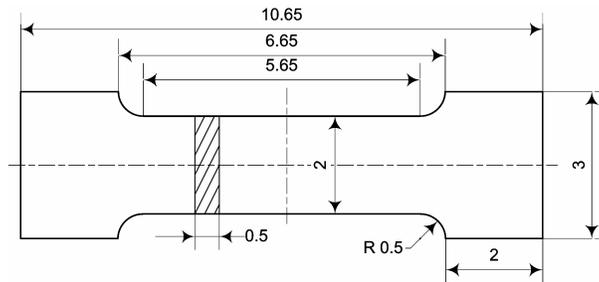
Figure 2.23. Miniaturised tensile test specimen

Cylindrical standard specimens and miniature specimens have been machined from the same samples extracted from different power plant components manufactured from different materials (Table 2.1). Fabrication and testing of cylindrical standard specimens (first series) have been performed in accordance with [54]. For the fabrication of the miniature specimens (second series) the method of punching has been initially used. A special fixture has been designed and manufactured for that goal (Figure 2.24). The third series of the specimens has been prepared by means of electrical discharge machining (EDM). Fabrication of this series of specimens have been performed in three stages: cutting of the plate

with 0.6–0.7 mm in thickness; grinding of the plate till the thickness of 0.5 mm; cutting of the specimen by EDM.
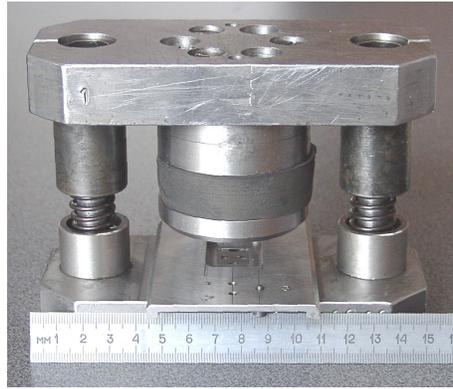
Figure 2.24. Device for miniature specimens
fabrication by punching

Tension tests of miniature specimens have been conducted on a manual test stand produced by Mecmesin Ltd company (Figure 2.25). For the force measurement a test stand is equipped by digital Basic Force Gauge BFG 1000 N. The receptiveness of the BFG is 0.1 N, the maximum force is 1000 N and standard error is $\pm 0.022\%$ with confidence level of 95%. Crosshead displacement is measured by IDS Digimatic Indicator with receptiveness of 0.001 mm. Both equipments are connected with computer and all data of the tension process can be

Figure 2.25. Manual test stand

registered and processed. The rate of the crosshead motion can be regulated by additionally equipped electromechanical drive (microstepping driver and gear). In accordance with standard [54] for the specimen with gauge length of 5.65 mm the strain rate shell be at the range of 0.085 –0.85 mm per minute. Preliminary tests have shown that changing the rate of the displacement within mentioned limits does not influence on the tensile test results. Nevertheless the constant rate of 0.4 mm per minute has been realised for basic tests.

For the gripping of the specimen and converting of the compressive force into the tension one a special reverser has been designed and manufactured (Figure 2.26). The grips of the reverser hold the specimen firmly and due to directing rods the uniaxial tension is realised.
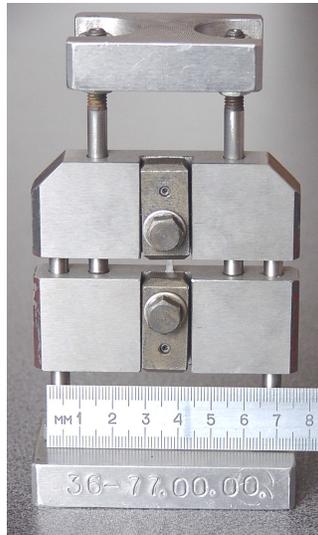
Figure 2.26. Reverser

Cylindrical standard specimens have been tested by testing machine Instron 8516.

2.4.2. Results

The results of tension tests are presented in Figure 2.27 and Table 2.4. The basic difference between stress-strain curves of standard and miniature specimens is the slope of the linear-elastic regime of the curves. The slope of the curves for miniature specimens is higher than for standard specimens. It is explained by insufficient rigidity and hence compliance of the test stand for tension of miniature

(a)

(b)

(c)
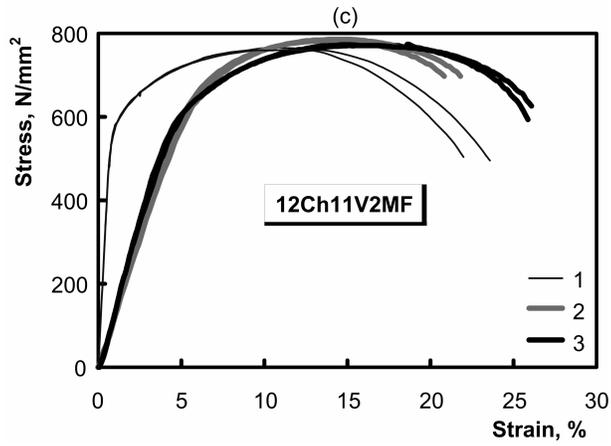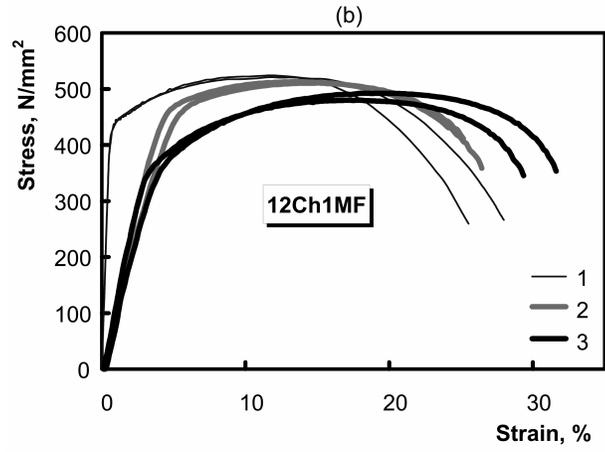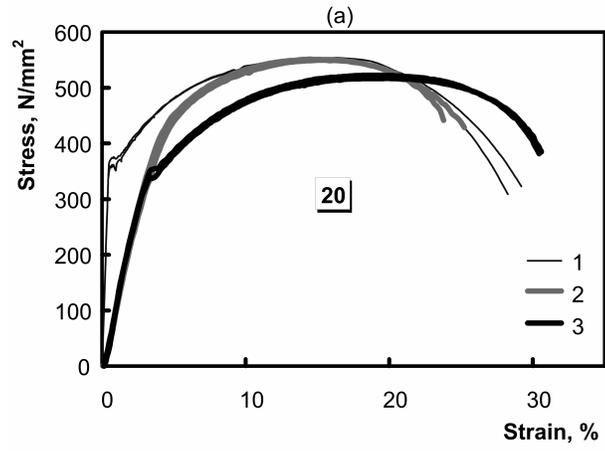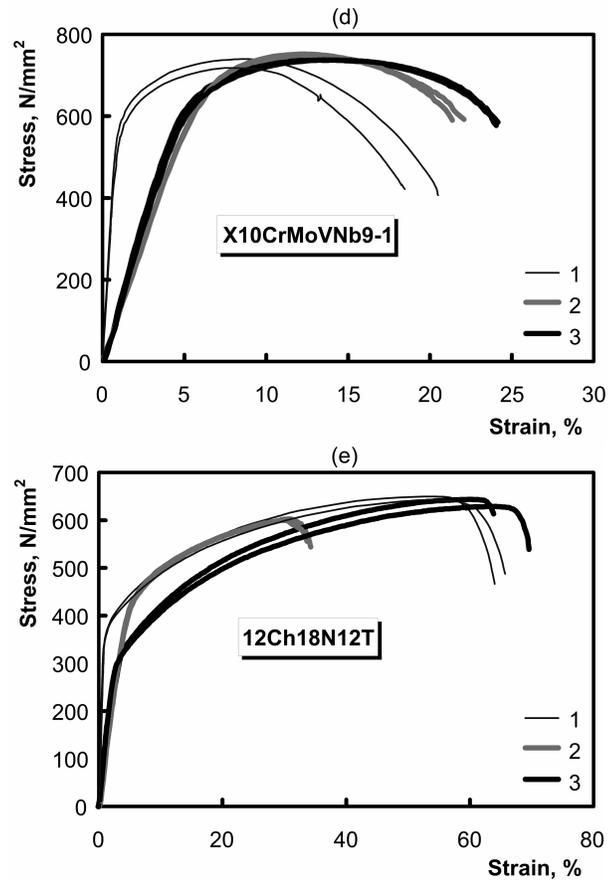
Figure 2.27. The results of the tension tests
1 – conventional cylindrical test specimens with standard size;
2 – miniature flat test specimens fabricated by means of punching;
3 – miniature flat test specimens fabricated by means of EDM

specimens. Thus the elongation to failure of the specimens has been determined individually by the drawing the line from fracture point and parallel to the elastic region of the stress-strain curve.

The analysis of the results has shown that percent elongation of the miniature specimens of the second series is essentially lower than percent elongation of standard specimens. At the same time the tensile strength and yield strength are in a quite good agreement. The main reason of that could be plastic deformation of the significant part (up to 2/3 of the cross section) of the miniaturised specimen during the fabrication process, namely during the punching. Such negative issue of reduced percent elongation has not been observed in tests of the third series of specimens, fabricated by EDM.

47

Table 2.4. The results of the tension tests

Steel grade	Symbol & Equation	Unit	Series		
			1^1	2^2	3^3
20	R_m	N/mm^2	554	550	520
	$R_{p0.2}$	N/mm^2	370	366	334
	$R_{p0.2}/R_m$		0.67	0.67	0.64
	A	%	29.0	20.6	27.1
	$1-R_m/R_m^1$		-	0.7%	6.2%
	$1-R_{p0.2}/R_{p0.2}^1$		-	1.1%	9.7%
	$1-A/A^1$		-	29.0%	6.3%
12Ch1MF	R_m	N/mm^2	522	512	486
	$R_{p0.2}$	N/mm^2	415	382	334
	$R_{p0.2}/R_m$		0.79	0.75	0.69
	A	%	27.3	22.3	27.2
	$1-R_m/R_m^1$		-	2.0%	6.9%
	$1-R_{p0.2}/R_{p0.2}^1$		-	7.8%	19.4%
	$1-A/A^1$		-	18.3%	0.4%
12Ch11V2MF	R_m	N/mm^2	774	784	773
	R_{p02}	N/mm^2	567	534	531
	$R_{p0.2}/R_m$		0.73	0.68	0.69
	A	%	23.8	15.8	21.6
	$1-R_m/R_m^1$		-	-1.4%	0.1%
	$1-R_{p0.2}/R_{p0.2}^1$		-	5.8%	6.4%
	$1-A/A^1$		-	33.6%	9.5%
X10CrMoVNb9-1	R_m	N/mm^2	742	750	737
	$R_{p0.2}$	N/mm^2	503	555	516
	$R_{p0.2}/R_m$		0.64	0.74	0.70
	A	%	19.6	16.7	19.8
	$1-R_m/R_m^1$		-	-1.0%	0.7%
	$1-R_{p0.2}/R_{p0.2}^1$		-	-10.3%	-2.7%
	$1-A/A^1$		-	14.9%	-1.1%
12Ch18N12T	R_m	N/mm^2	653	601	636
	$R_{p0.2}$	N/mm^2	316	361	284
	$R_{p0.2}/R_m$		0.47	0.60	0.45
	A	%	65.2	28.2	66.8
	$1-R_m/R_m^1$		-	7.9%	2.6%
	$1-R_{p0.2}/R_{p0.2}^1$		-	-14.1%	10.1%
	$1-A/A^1$		-	56.7%	-2.4%

[1] – conventional cylindrical test specimens with standard size;
[2] – miniature flat test specimens fabricated by means of punching;
[3] – miniature flat test specimens fabricated by means of EDM.

The comparison of the tests results has shown that the disagreement between the tests results of the first and third series is minimal and does not exceed 10% (with the exception of the yield strength of the steel 12Ch1MF; in this case the disagreement is 19.4%). The analysis of standard deviation of the conducted tests has shown the high repeatability of the results (Table 2.5). In particular tests, the standard deviation of the miniature specimens testing results is even less than for standard specimens that is consequence of the reliability of the miniature specimens testing.

Table 2.5. Standard deviation of the mechanical properties determination

Steel grade	Symbol	Unit	Series		
			1	2	3
20	R_m	N/mm^2	4.3	1.3	4.0
	$R_{p0.2}$	N/mm^2	2.3	12.8	8.8
	A	%	0.7	1.3	0.0
12Ch1MF	R_m	N/mm^2	2.8	1.8	8.9
	$R_{p0.2}$	N/mm^2	6.8	2.1	5.1
	A	%	1.8	1.6	1.0
12Ch11V2MF	R_m	N/mm^2	0.6	2.4	2.7
	$R_{p0.2}$	N/mm^2	5.4	6.1	0.4
	A	%	1.7	0.4	0.1
X10CrMoVNb9-1	R_m	N/mm^2	2.9	3.0	0.4
	$R_{p0.2}$	N/mm^2	4.2	12.0	2.8
	A	%	1.5	0.5	0.2
12Ch18N12T	R_m	N/mm^2	6.0	2.0	10.6
	$R_{p0.2}$	N/mm^2	11.2	4.4	0.3
	A	%	1.4	0.5	2.2

Thus in order to minimise the size of extracted sample and hence to get mechanical0. properties of the metal of the investigated power plant component in service the technique of miniature flat specimens testing has been developed. The results of the tests of miniaturised specimens fabricated by punching have shown a good agreement with the standard specimens testing results with exception of the percent elongation, which has been significantly lower due to plastic deformation during punching in fabrication process. The results of the tests of miniature specimens prepared by means of electrical discharge machining have shown the best agreement with the results of standard specimens testing. Moreover, the high repeatability of the results of tests of miniature specimens has been observed. Thus, the technique of the miniature flat specimens testing is an accurate and reliable method and could be definitely used for the evaluation of the tensile properties of the metal.

3. ASSESSMENT OF REMAINING LIFE OF THE METAL IN THE CONDITIONS OF HIGH TEMPERATURE CORROSION

The metal of steam boilers heating surfaces such as superheater and reheater in addition to creep undergoes high temperature corrosion (HTC). This issue is highly significant for oil shale boilers. The Estonian oil shale is one of the most complicated fossil fuels. In the process of the oil shale combustion inorganic matter produces several chemically active compounds leading to both fouling and accelerated HTC of heating surfaces tubes. The acceleration of the corrosion process is caused mainly by the presence of alkali metals chlorides in the oil shale ash. The influence of chlorides on the corrosion of steels has been studied in many researches [55–59].

Thus, the tubes of superheater and reheater of oil shale steam boilers are subject to intensive corrosion and metal damage due to HTC is much higher than creep damage. It is therefore highly significant in condition assessment of the metal of steam boilers heating surfaces to take into account the metal loss due to HTC.

A detailed investigation of HTC of different boiler steels under impact of oil shale ash was carried out over the past four decades [60–68]. Despite the fact, that many of boiler steels have been investigated, the "ideal" steel, that could be operated at elevated temperatures in the presence of oil shale ash deposits for a long time, has not yet been revealed up to the present. Therefore, in order to reveal the most corrosion-resistant and most suitable for operation in the conditions of HTC under influence of oil shale deposits the research of different new steels is always of high importance. The detailed review of laboratory HTC tests of several austenitic steels is presented in [I].

3.1. Laboratory tests

The laboratory corrosion tests of austenitic steels B-407, X8CrNiNb16-13 and X8CrNiMoNb16-16 have been carried out in accordance with standard techniques [69, 70]. These tests have been performed in electrically heated vertical tube-type furnaces with an inner diameter of 40 mm (Figure 3.1). The combustion products of natural gas have been directed into the furnaces by the pipe header. The combustion gas velocity in the furnaces has been 0.15–0.18 m/s. In order to avoid condensation of water vapour the pipe header has been heated by electrical heating coils. The temperature in the furnaces has been maintained at 540 °C, 580 °C and 620 °C with accuracy ±2 °C.
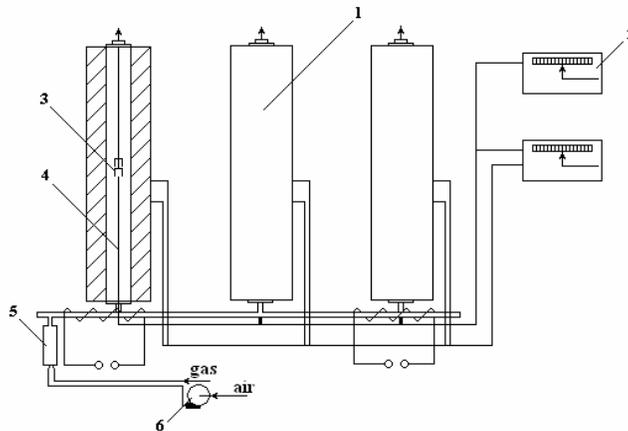
Figure 3.1. The laboratory unit for investigation of high temperature corrosion of metals. 1 – electrical furnaces; 2 – tools for temperature measurement and control; 3 – test specimens; 4 – thermocouples; 5 – combustion chamber; 6 – fan

The corrosion tests have been performed on flat polished specimens with dimensions 3x10x40 mm (Figure 3.2), which have been cut from original boiler tubes. Chemical compositions of examined steels are presented in Table 2.1. Prior to the tests all specimens were degreased, precisely measured and weighed. They were then coated with a mixture of oil shale ash and ethyl alcohol for imitation of oil shale on-tube deposits. Electrical precipitator ash, with chlorine content of about 0.5%, was used in the laboratory experiments. The full chemical composition of the Estonian oil shale ash used in corrosion tests is as follows, wt.%: SiO_2 28.4; Fe_2O_3 3.66; Al_2O_3 14.46; CaO 32.02; MgO 3.78; SO_3 9.91; K_2O 6.71; Na_2O 0.56; Cl 0.5.
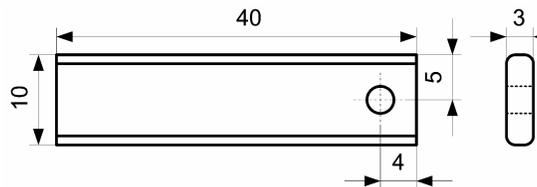
Figure 3.2. Test specimen

The removal of corrosion and oxide scales from the post-test specimens was performed in the environment of liquid sodium by blowing ammonia [71]. The quantity of corroded material was determined as the difference of mass of clean

specimens before and after testing. The accuracy of weighing was ±0.1 mg. On the basis of mass difference the corrosion depth was calculated ($\Delta S'$, mm).

3.2. Industrial tests

Heating surfaces of oil shale boilers are subjected to severe fouling by ash deposits, which reduce heat transfer and need to be periodically removed. Therefore cleaning of tubes from ash deposits is realised. At the same time cleaning forces can cause total or partial destruction of the oxide scale on the tubes surface. Oxide scale could be also destructed by thermal shock due to rapid fluctuations in boiler operating loads, or weight of deposits. It leads to rapid acceleration of the corrosion rate of the metal due to corrosion of a clean metal surface without any oxide scale. Thus in order to take into account the effect of possible destruction of the oxide scale on total corrosion process the field tests of the investigated steels should be realised.

Industrial corrosion tests of austenitic steels B-407, X8CrNiNb16-13 and X8CrNiMoNb16-16 have been carried out in the oil shale pulverised firing boilers at Narva Power Plants in Estonia. The duration of the tests has been varied in the range of 5 to 25 thousands hours and the metal temperature 503–520 °C.

3.3. Results

The results of laboratory tests are presented as kinetic diagrams of corrosion depth of examined steels in coordinates $\ln\Delta S' - \ln\tau$ (Figure 3.3).

In logarithmic coordinates the kinetic lines of high temperature corrosion are straight lines and usually expressed by following empirical correlation:

$$\ln \Delta S' = \alpha - \beta T^{-1} + (\gamma + \varepsilon T)\ln \tau, \qquad (3.1)$$

where:

α, β, ε, γ – coefficients depending on ash characteristics of the particular fuel, grade and temperature of the metal. Binominal ($\gamma + \varepsilon \cdot T$) is usually defined as exponent of corrosion process. All these coefficients are determined experimentally.

On the basis of the tests results the following empirical equations for prediction of corrosion depth of the investigated steels depending on operational time τ and metal temperature T have been established:

B-407 $\qquad \ln(\Delta S')=-3.5-3077/T+(-1.11+1.84\cdot10^{-3}\cdot T)\ln\tau,$ (3.2)

X8CrNiNb16-13 $\quad \ln(\Delta S')=-6.0-620/T+(-1.12+1.8\cdot10^{-3}\cdot T)\ln\tau,$ (3.3)

X8CrNiMoNb16-16 $\ln(\Delta S')=-13.5+4027/T+(-0.97+1.8\cdot10^{-3}\cdot T)\ln\tau.$ (3.4)
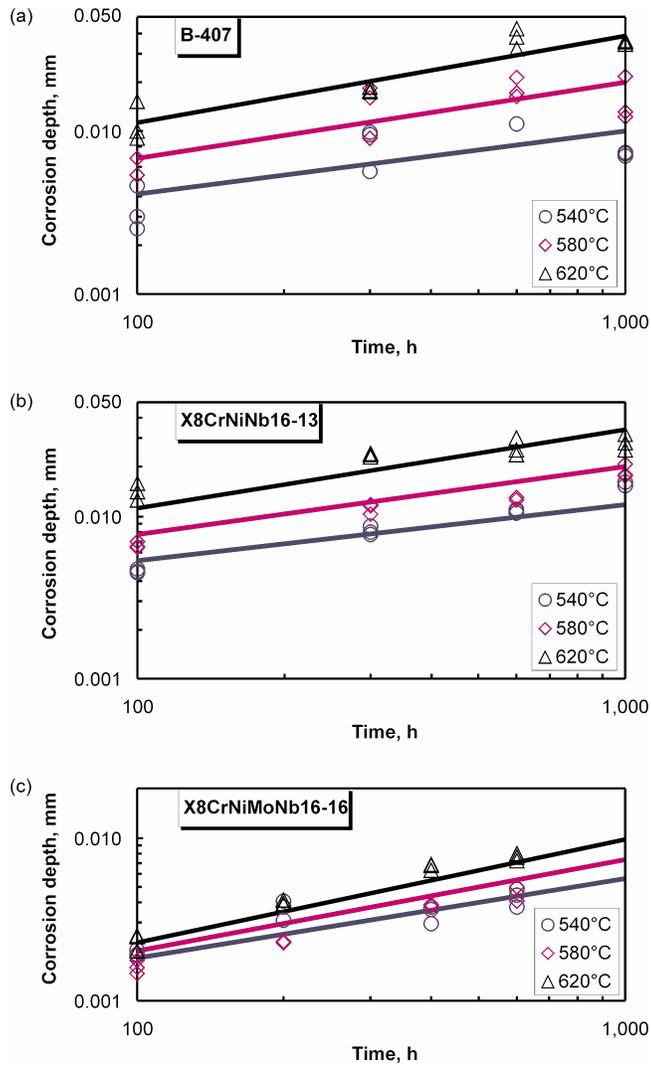
Figure 3.3. The results of HTC laboratory tests in the presence of
Estonian oil shale ash

Comparative analysis of results of laboratory HTC testing of investigated austenitic steels and results of previously performed investigations of other steels which are used for manufacturing of superheater tubes has been carried out and could be performed by means of Figure 3.4. The analysis has shown that for the time being the best corrosion resistant steel in conditions of laboratory tests is X8CrNiMoNb16-16. This conclusion is valid for all investigated temperatures (540–620 °C).
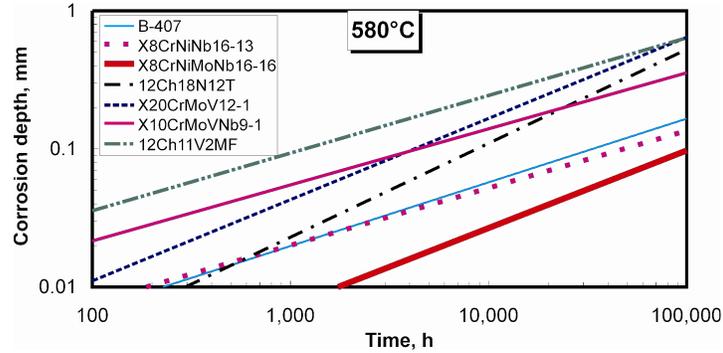
Figure 3.4. The results of HTC laboratory tests of different boiler steels
in the presence of oil shale ash

These results have been obtained by the corrosion tests under stable layer of the oil shale ash deposits, however the periodic destruction of the oxide scale that occurs in the real boiler conditions sharply accelerates the corrosion. Thus the final form of equation for prediction of the high temperature corrosion in the presence of oil shale ash could be established only after industrial tests in the real boiler conditions.

In the conditions of cyclic damage of the oxide scale on a metal surface the HTC depth could be calculated as [59]:

$$\Delta S_o = \left[1 + \xi\left(B \cdot m^{1-n} - 1\right)\right] \cdot \Delta S', \text{ mm.} \tag{3.5}$$

The loss of oxide scale adhesion and its spalling have been observed for the steel X8CrNiNb16-13 [67]. It has been found that the total destruction of the oxide scale (ξ=1) takes place in every cycle of cleaning heating surfaces and shutdown of boiler. The investigations of the oxide scale on the tested tubes from the steels B-407 and X8CrNiMoNb16-16 have shown it to be dense and bounded well with the metal (ξ<0.35).

3.4. Method for estimation of remaining life of superheater tubes

As it was outlined above superheater surfaces in oil shale steam boilers undergo intensive HTC, which causes reduction of wall thickness that effectively increases stresses through the thinned wall. It leads to reduction of lifetime of superheater tubes and results in the necessity of superheater repair every 3–4 years with replacement of up to 30–50% of austenitic tubes. In order to reduce the amount and cost of repair and to avoid unscheduled outages due to tubes failure the method of assessment of remaining life for superheater austenitic steel tubes operating in

54

conditions of intensive HTC has been developed. The main point and application examples of the developed method are presented in detail in [II].

The method is based on the calculation of allowable reduction of tube wall thickness. Firstly the minimum required wall thickness of tubes should be calculated as follows [72]:

$$S = \frac{p \cdot D_i}{2f \cdot z - p}, \text{mm.} \tag{3.6}$$

Allowable reduction of wall thickness than can be obtained as:

$$\Delta S_{allowable} = \frac{S_0 - S - \Delta S_{igc}}{1.3} - 0.1, \text{mm,} \tag{3.7}$$

where 1.3 is safety factor which accounts the difference in corrosion depth along the perimeter of the tube and 0.1 is loss of wall thickness due to polishing of the tube surface prior to measurement of thickness, mm.

The next step of the remaining life prediction is estimation of the wall thickness loss due to HTC on the outside (fire-side) and inside (steam-side) surfaces of the tube. Fire-side corrosion depth of the tube ΔS_0 is a function of operation time τ, ash characteristics of the fuel, grade and temperature of the metal and amount of periodic cycles of oxide scale partial or entire destruction m and could be found by (Eq. 3.5). Steam-side corrosion depth of the tube ΔS_i depends on operation time τ, grade and temperature of the metal and is calculated by using empirical equation that is similar to (Eq. 3.1)..

So, the total corrosion depth of the tube is:

$$\Delta S = \Delta S_o + \Delta S_i, \text{mm.} \tag{3.8}$$

Prediction of remaining life of tubes consists in drawing a kinetic diagram of corrosive resistance of steel according to (Eq. 3.8) (for various amounts of periodic destructions of the oxide scale $m = \tau / \tau_0$, where τ_0 – period of time between destructions of the oxide scale). Also the line defining the allowable reduction of the tube wall thickness depending on operation time should be plotted on the diagram. Such diagram for austenitic steel 12Ch18N12T (metal temperature T=580 °C, the content of chlorine in oil shale ash – 0.5%) is represented in Figure 3.5. Then the values of corrosion depth of the tubes (determined on the basis of wall thickness measurement) should be depicted on the diagram. Ideally the point of real value of corrosion depth should be on the line of corrosion depth prediction depending on time at point A_1 and corresponding operation time τ_1 (Figure 3.5). In this case the point A_2 and corresponding time τ_2 define the lifetime

of the tube (or the time when the tube wall thinning reaches the maximum allowable value $\Delta S_{allowable}$), and (τ_2-τ_1) – remaining life of the tube.

If actual operation time τ'_1 is less than predicted time (that could be caused by the difference between calculation and real conditions of tube operation), in order to determine the remaining life, the line from point B_1 and parallel to the line of corrosion depth prediction should be drawn. New point B_2 defines the lifetime of the tube and the remaining life, in this case, is (τ'_2-τ'_1). Similarly the remaining life should be determined if actual operation time is longer, than predicted time, point C_1. In this case, the remaining life is (τ''_2-τ''_1).
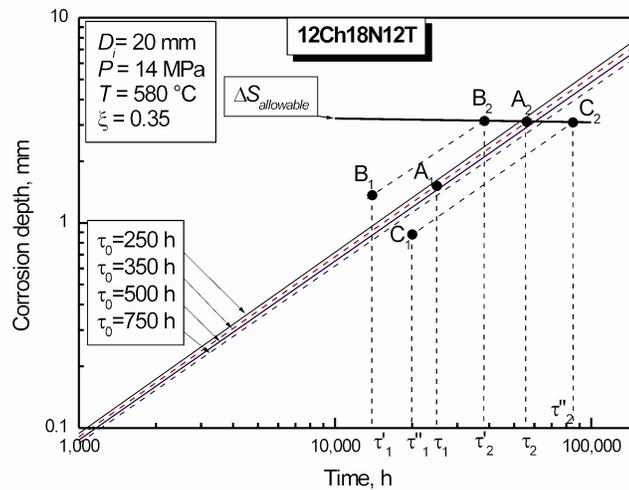
Figure 3.5. Diagram for prediction of remaining life of austenitic
steel 12Ch18N12T in an oil shale boiler

Remaining life estimation on the basis of actual corrosion depth data determined on the basis of measurement of tube wall thickness could increase the accuracy of prediction. In this case actual conditions of corrosion such as metal temperature, aggressiveness of corrosive environment, the degree of oxide scale destruction etc. are taken into account integrally. Thus the use of the proposed method allows significantly to increase the accuracy of prediction of remaining life thanks to eliminating uncertainty of corrosion conditions.

4. CONCLUSIONS

1. Applicability analysis of tensile properties determination of power plant steels by means of indirect techniques on the basis of hardness has been performed. The results of analysis have shown that the considered indirect techniques could not substitute the direct tests and the tensile properties of the actual material can be accurately and reliably obtained only by means of direct testing.

2. The impact of the dimple on stress distribution in pipes and turbine rotor has been analysed applying finite elements method. It has been found that metal sampling by means of designed in Tallinn University of Technology sampling machines does not lead to initiation of inadmissible stress concentrations and could be used without sacrificing of the safety of the in-service components and does not require the sampled area to be repaired. The designed sampling devices have been successfully implemented in power plants of Estonia. Totally more than 200 samples from external surface of steam pipes, turbine casings, drums and internal surface of turbine rotors have been extracted so far.

3. In order to analyse the applicability of the determination of tensile properties of the power plant components material applying small punch testing technique the physical and numerical experiments have been carried out. The comparison of results of small punch tests and conventional standard cylindrical specimens tensile tests has shown that tensile strength of the metal can be easily obtained as a linear function of the maximum punch force determined in the small punch test. The finite element model of the punch process has been also built and results of finite element modelling have shown quite good agreement with physical experiments. On the basis of experiments and finite element model it has been found that yield strength of the metal could not be determined with sufficient accuracy using of small punch tests.

4. The technique of the miniature flat specimens has been developed for determination of the metal tensile properties. The results of tests have shown high repeatability and good agreement with results of standard specimens testing. Thus, the developed technique of the miniature flat specimens testing is an accurate and reliable method and could be definitely used for the evaluation of the tensile properties of the metal.

5. Laboratory and industrial high temperature corrosion tests of several austenitic steels have been performed in order to reveal the most corrosion-resistant and most suitable one for operation in the conditions of creep, high temperature corrosion under influence of oil shale ash deposits and cyclic oxide scale destruction. The results have shown that for the time being the best corrosion resistant steel is X8CrNiMoNb16-16.

6. The method of assessment of remaining life for superheater austenitic steel tubes operating in conditions of intensive high temperature corrosion has been developed. This technique allows to reduce the amount and cost of repair and to avoid unscheduled outages due to tubes failure.

REFERENCES

1. VGB-R 509 L Widerkehrende Prüfungen an Rohrleitungsanlagen in fossilbefeuerten Wärmekraftwerken. 1984 (in German).
2. EN 10291:2001 Metallic Materials – Uniaxial Creep Testing in Tension Method of Test.
3. GOST 3248-81 Metals – Method of Creep Test, Moscow, 1981 (in Russian).
4. GOST 10145-81 Metals – Method of Creep Rupture Test, Moscow, 1981 (in Russian).
5. Hertzberg R. W. Deformation and Fracture Mechanics of Engineering Materials 4th ed. New York: John Wiley and Sons, Inc., 1996, p. 786.
6. Dowling N. E. Mechanical Behavior of Materials. New Jersey: Prentice Hall, 1999, p. 830.
7. Antikain P. Metals and Stress Calculation of Boilers and Piping. Moscow: Energia, 1990, p. 424 (in Russian).
8. Kumanin V., Kovalyova L., Aleksejev S. Durability of Metal in the Conditions of Creep. Moscow: Energia, 1988, p. 224 (in Russian).
9. Residual Life Assessment and Microstructure, ed. Concari S. ECCC recommendations, Vol. 6 (1), ETD, 2005.
   http://www.ommi.co.uk/etd/eccc/advancedcreep/V6i1x.pdf (18.09.2007)
10. OST 34.70.690-96 Metal of Power Plant Equipment. Methods of Metal Structure Analysing in the Conditions of Operation. Appendix G. 1996 (in Russian).
11. VGB-TW 507/TW507e Guideline for the Assessment of Microstructure and Damage Development of Creep Exposed Materials for Pipes and Boiler Components, 1992.
12. Auerkari P., Borggreen K., Salonen J. Reference micrographs for evaluation of creep damage in replica inspections. – NT Technical Report 170, Nordtest, Espoo, 1992.
13. Permikin V. Mechanism of damage of steel at high temperature creep, *In:* Proc. of Conf. "Metal of Thermal Power Plant equipment. Problems and Perspectives, 30 Oct.–02 Nov., 2006, VTI, Moscow, Russia (in Russian).
14. Recommendations for data acceptability criteria and the generation of creep data, ed. by Gariboldi E. and Brett S. ECCC recommendations, Vol. 3 (I), ETD, 2005.
   http://www.ommi.co.uk/etd/eccc/advancedcreep/V3PIi5x.pdf (18.09.2007).
15. Zlepko V., Shvetsova T., Linkevich K. The Long-Term Strength of the Metal of Steam Line Tubes Made from Cr-Mo-V Steel after Their Service at a Thermal Power Station. Thermal Engineering Vol. 46, No. 5, 1999, p. 366.
16. Krutasova E., Reliability of Power Equipment Metal. Moscow: Energoatomizdat, 1981, p. 240 (in Russian).
17. Berezina T., Bugay N., Trunin I. Diagnosis and Prognosis of Power Equipment Metal Life. Kiev: Tehnika, 1991, p. 119 (in Russian).

18. Berezina T. Key to Steels and Alloys in Thermal Engineering. Handbook, Chelyabinsk, 2004 (in Russian).
19. Ray A.K., Tiwari Y.N., Sinha R.K., Chaudhuri S., Singh R. Residual life prediction of service exposed main steam pipe of boilers in a thermal power plant. Engineering Failure Analysis 7, 2000, pp. 359–376.
20. Nakoneczny G. J., Schultz C. C. Life assessment of High Temperature Headers. Babcock and Wilcox, 1995.
21. Cheruvu N.S. Degradation of mechanical properties of Cr-Mo-V and 2.25 Cr-1Mo steel components after long-term service at elevated temperatures. Metallurgical Transactions, Vol. 20A, No. 1, Jan, 1989, pp. 87–97.
22. Smirnova A., Balashov Y., Tikhonova T., Ivanova L. Degradation of Structure and Mechanical Properties of Steel 20 During Long-Term Operation at Temperatures Higher than 450 °C. Teploenergetika, 1993 No. 11, pp. 11–13 (in Russian).
23. SO 153-34.17.421 (RD 10-577-03) Instruction of Metal Control and Life Extension of Basic Components of Boilers, Turbines and Piping at Power Plants, 2003 (in Russian).
24. Instruction of Mechanical Properties and Impact Toughness Determining of Power Plant Equipment Metal by Non-Destructive Testing. SMiS "Donbassenergo", 1978 (in Russian).
25. Methodical Instructions of Hardness and Mechanical Properties Determining of Low Alloyed Steels of Power Equipment without Specimens Testing, Ural VTI, 1978 (in Russian).
26. Haggag F., Murty K. A Novel Stress-Strain Microprobe for Nondestructive Evaluation of Mechanical Properties of Materials. Nondestructive Evaluation and Materials Properties III, The Minerals, Metals & Materials Society, 1997, pp. 101–106.
27. Purmensky J., Kupka V., Stanoveni užitnych vlastnosti hutnich a strojirenskych vyrobku pomoci metod velmi malych vzorku. Hutnichke listy, 48, 1993, pp. 65–69 (in Czech).
28. Data acceptability criteria and data generation: recommendations for creep testing of post exposed (ex-service) materials, ed. by E Gariboldi and S Brett. ECCC recommendations, Vol. 3 (III), ETD, 2003.
    http://www.ommi.co.uk/etd/eccc/advancedcreep/V3PIIIi4x.pdf (21.05.05).
29. Srivastav S. Foulds J. R., Andrew S. P., *et al.* Unit-specific evaluation of steam turbine rotors using miniature sample removal and safer-pc
    http://www.exponent.com/about/docs/esia2000.pdf (21.03.06).
30. Torsello G., Cesi ct elettrotecnico sperime, Apparatus for taking samples of conducting material, patent number: EP1413872, 2004.
31. Sarandi J., Tallermo H., Klevtsov I., Uus M. Device for Cutting Samples from Metal Surface, Estonian Utility model EE00492, IPC B24B 19/00, B23B 47/18, Published 17.02.2005.

32. Klevtsov I., Neshumayev D., Uus M. Control Panel for the Device for Cutting Samples from Metal Surface. Estonian Utility model EE00527 U1, IPC B23Q 15/08, B24B 19/00, Published 15.07.2005.

33. Manahan M., Argon A., Harling O. The development of a miniaturised disk bend test for the determination of post-irradiation mechanical properties. J. Nucl. Mater., 1981, 103–104, pp. 1545–1550.

34. Fleury E., Ha J. S. Small punch tests to estimate the mechanical properties of steels for steam power plant. I. Mechanical strength. II. Fracture toughness. Int. J. Pressure Vessels Piping, 1998, No. 75, pp. 699–713.

35. Parker J., Stratford G., Shaw N., *et al.* The application of miniature disc testing for the assessment of creep damage in CrMoV rotor steel, Conf. Proc. BALTICA IV, Vol. 2, 1998, pp. 477–488.

36. Brookfield D., Li W., Rodgers B., *et al.* Material properties from small specimen using the punch and bulge test. J. Strain Analysis, 1999, Vol. 34, No. 6, pp. 423–435.

37. Husain A., Sehgal D., Pandey R., Design of a simple, versatile, small-specimen punch test setup for determination of the mechanical behavior of materials, Experimental Techniques, 2002.

38. Ruan Y., Spätig P., Victoria M. Assessment of mechanical properties of the martensitic steel EUROFER97 by means of punch tests. J. Nucl. Mater., 2002, Vol. 307-311, pp. 236–239.

39. Campitelli E., Spätig P., Bonadé R., *et al.* Assessment of the constitutive properties from small ball punch test: experiment and modelling. J. Nucl. Mater., 2004, Vol. 335 (3), pp. 366–378.

40. Milička K., Dobeš F. Small punch testing of P91 steel, Int. J. Pressure Vessels Piping, 2006, No. 83, pp. 625–634.

41. Egan P., Whelan M., Lakestani F., *et al.* Small punch test: An approach to solve the inverse problem by deformation shape and finite element optimization, Comput. Mater. Sci. (2006), doi:10.1016/j.commatsci.2006.10.021.

42. Tettamanti S., Crudeli R. Small punch creep test: a promising methodology for high temperature plant components life evaluation, *In:* Proc. Baltica IV, Vol. 1, pp. 251–259, Helsinki-Stockholm-Helsinki, 7–9 September, 1998.

43. Yang Z., Wang Z-W. Relationship between strain and central deflection in small punch creep specimens, Int. J. Pressure Vessels Piping, 2003, No. 80, pp. 397–404.

44. Bicego V., Di Persio F., Hurst R., *et al.* Comparability of results via the miniaturised small punch creep test method and traditional uniaxial creep testing, *In:* Proc. 11th Int. Conf. on Fracture, Turin, Italy, 20–25 March, 2005. http://www.icf11.com/proceeding/EXTENDED/5025.pdf (20.09.2007).

45. Stratford G., Di Persio F., Klaput J. Miniaturised creep testing using the small punch (SP) test technique, *In:* Proc. 11th Int. Conf. on Fracture, Turin, Italy, 20–25 March, 2005. http://www.icf11.com/proceeding/EXTENDED/4175.pdf (20.09.2007).

46. Šturm R., Li Y. Small-punch testing of a weld's heat-affected zones, Materiali in Technologije, No. 40(2), 2006.
http://ctklj.ctk.uni-lj.si/kovine/izvodi/MIT062/sturm.pdf (20.09.2007).

47. Hurst R., Bicego V., Foulds J. Small punch testing for creep – progress in Europe, *In:* Proc. 8th Int. Conf. on Creep and Fatigue at Elevated Temperatures, San Antonio, Texas, USA, 22–26 July, 2007.
http://www.clarusllc.com/files/Download/CREEP2007-26693.pdf
(20.09.2007).

48. Foulds J., Parnell T., Woytowitz P., *et al.* Fracture toughness by small punch testing, ASTM J. Testing Evaluation, Vol. 23 (1), 1995, pp. 3–10.

49. Bulloch J. The small punch assessment of toughness losses in low alloy steels, *In:* Conf. Proc. BALTICA IV, Vol. 2, pp. 489–498, Helsinki-Stockholm-Helsinki, 7–9 September, 1998.

50. Abendroth M., Kuna M. Identification of ductile damage and fracture parameters from the small punch test using neural networks, Eng. Frac. Mech., 2006, No. 73, pp. 710–725.

51. Manahan M., Browning A., Argon A., *et al.* The use of small-scale specimens for testing irradiated material, ASTM-STP 888, American Society for Testing and Materials, Philadelphia, PA, 1986.

52. Wegst C. Key to Steel. Verlag Stahlschlüssel Wegst GMBH, 1998.

53. ANSYS Release 9.0 Documentation.

54. EN 10002-1:2001 Testing of Metallic Materials. Method of Test at Ambient Temperature.

55. Baxter L., Nielsen H. The effect of fuel-bound chlorine and alkali on corrosion initiation, Prepr. Pap. Am. Chem. Soc., Div. Fuel Chem., 1997, Vol. 42, No. 4. pp. 1091–1095.

56. James P., Pinder L. Effect of coal chlorine on the fireside corrosion of boiler furnace wall and superheater/reheater tubing, Mater. High Temperature. 1997, Vol. 14, No. 3, pp. 187–196.

57. Nielsen H., Frandsen F., Dam-Johansen K., *et al*. The implications of chlorine-associated corrosion on the operation of biomass-fired boilers. Prog. in Energy and Combust. Sci., 2000, 26, pp. 283–298.

58. Uusitalo, M., Vuoristo, P., Mäntylä T. High temperature corrosion of coatings and boiler steels below chlorine-containing salt deposits, Corrosion Science, 2003, 46 (6), pp. 1311–1331.

59. Ots A. Oil Shale Fuel Combustion, Tallinn, 2006, p. 833.

60. Arro, H., Tallermo, H., Tomann, E., Öpik, I. About method of laboratory research of thermal resistance of boiler steels in conditions of burning Baltic oil shale, Abst. of conf. about processes in mineral matter of power engineering fuels, Tallinn: TUT, 1969, pp. 47–53 (in Russian).

61. Ots, A., Tallermo, H., Tomann, E. Influence of initial ash deposits on high-temperature corrosion of boiler steels, Teploenergetika, 1972, No. 1, pp. 22–25 (in Russian).

62. Tallermo, H., Ots, A.The influence of the deposits on the high temperature corrosion of the super heaters of oil shale fired boilers, Transactions of TUT, 1973, No. 339, pp. 3–12 (in Russian).
63. Ots, A., Paist, A. Laboratory investigation of high-temperature corrosion of boiler alloys under the impact of Estonian oil shale ash, Oil Shale, 1997, Vol. 14, No. 3, Special, pp. 236–245.
64. Tallermo, H., Lausmaa, T., Klevtsov, I., Nuutre, M. The influence of chlorine in ash deposits on 12Cr1MoV alloy high temperature corrosion, Oil Shale, Tallinn, 1997, Vol. 14, No. 3, pp. 307–316.
65. Tallermo, H., Tomann, E., Klevtsov, I., Bojarinova, T., Nuutre, M. Corrosion resistance of ferritic alloys 13 CrMo 44 and 10 CrMo 910 in conditions of superheaters of pulverized oil shale boiler, Oil Shale, 1997, Vol. 14, No. 3 Special, pp. 317–327.
66. Tallermo, H., Klevtsov, I., Uus, M. Peculiar high temperature corrosion of martensite alloy under impact of Estonian oil shale fly ash, *In:* Proc. Baltica IV, Helsinki-Stockholm-Helsinki, 7-9 Sept. 1998, Vol. 1, pp. 295–303.
67. Klevtsov, I., Tallermo, H., Bojarinova, T., Lausmaa, T. High-temperature corrosion resistance of the austenitic steels in the presence of chlorine-containing on-tube deposits, Oil Shale, Tallinn, 2003, Vol. 20, No. 4, pp. 501–509.
68. Klevtsov, I., Tallermo, H., Bojarinova, T., Crane, R. A., High, A. Temperature corrosion resistance of boiler steels in the presence of chlorine-containing surface deposits, ASME Journal of Pressure Vessel Technology, Boston, 2005, Vol. 127, No. 2, pp. 106–111.
69. RTM 108.030.116-78 Standards for Determination of Corrosive Resistance of Boiler Alloys at Elevated Temperatures (in Russian).
70. OST 108.030.01-75 Steam Boilers. Method of Corrosion Tests, Moscow, 1973 (in Russian).
71. Antikain P. Corrosion of Steam Generator Metals. Energia, Moscow, 1977 (in Russian).
72. EN 13480-3 Metallic Industrial Piping. Part 3: Design and Calculation. 2002.

ASSESSMENT OF METAL CONDITION AND REMAINING LIFE OF IN-SERVICE POWER PLANT COMPONENTS OPERATING AT HIGH TEMPERATURE

ABSTRACT

Thesis is devoted to the problems of metal condition and remaining life assessment of in-service power plant components. In the given work the influence of long-term operation at high temperature on short-term mechanical properties has been analysed on the basis of literature. The results of analysis have shown that during service time the decrease of short-term mechanical properties takes place.

It has been found that indirect techniques of tensile properties determination of power plant steels on the basis of hardness could not substitute the direct tests and the tensile properties of the actual material can be accurately and reliably obtained only by means of direct testing.

Two sampling devices for extraction of small metal samples from in-service power plant components have been designed and manufactured. On the basis of finite element modelling results it has been found that metal sampling by means of designed machines could be used without sacrificing of the safety of the components and does not require the repair of the sampled area.

In order to analyse the applicability of tensile properties determination by means of small punch testing technique the number of physical and numerical experiments have been performed. The results have shown that tensile strength of the metal can be easily obtained as a linear function of the maximum punch force. However, it has been found that yield strength of the metal could not be determined with sufficient accuracy using small punch tests.

The technique of the miniature flat specimens has been developed. The results of tests have shown the developed technique to be an accurate and reliable method for the determination of the tensile properties of the metal.

Laboratory and industrial high temperature corrosion tests carried out within the present study have revealed that the most suitable steel for operation in the conditions of high temperature corrosion under influence of Estonian oil shale ash deposits is X8CrNiMoNb16-16.

The method of remaining life assessment for superheater tubes operating in conditions of intensive high temperature corrosion has been developed. Using of this technique allows to reduce the amount and cost of repair and to avoid unscheduled outages due to tubes failure.

Above-mentioned results of the present study and developed techniques are very important and successfully implemented for metal condition and remaining life assessment of Estonian power plant components.

ELEKTRIJAAMADE KÕRGETEMPERATUURSETE SEADMETE METALLI SEISUNDI JA JÄÄKRESSURSI HINDAMINE

KOKKUVÕTE

Narva elektrijaamade põhiseadmed on käesolevaks ajaks töötanud juba 200–250 tuhat tundi ja nende ressurss on ammendumas. Edaspidise ohutu ekspluatatsiooni tagamiseks on väga oluline osata hinnata seadmete ressursikulu võimalikult täpselt ja määrata lubatud tööaeg järgmise kohustusliku metalli kontrollini. See võimaldab metalli kontrolli tähtaegu ja mahte optimeerida ning vältida suuri avariisid ja nendega seotud võimalikke inimohvreid ja purustusi. Seega uuringute tähtsust energiaseadmete töökindluse valdkonnas ei ole võimalik ülehinnata.

Antud töö on pühendatud energiaseadmete metalli seisundi uuringute ja jääkressursi määramise probleemidele. Soojuselektrijaamade põhilised elemendid töötavad roomavuse tingimustes. Kirjanduse alusel on töös analüüsitud toatemperatuuril määratud lühiajaliste mehaaniliste omaduste muutumist ekspluatatsiooni käigus. Analüüsi tulemused näitasid, et metalli pikaajaline ekspluatatsioon roomavuse tingimustes viib metalli lühiajaliste mehaaniliste omaduste halvenemisele ja struktuuri kahjustusele ning energeetiliste seadmete komponentide eluea lühenemisele. Seetõttu on seadmete ohutu käitamise ja ressursikulu hindamiseks hädavajalik ekspluateeritavate elementide metalli mehaaniliste omaduste ja struktuuri perioodiline kontroll.

Töös on vaadeldud mehaaniliste omaduste määramise kaudseid meetodeid ja leitud, et lühiajaliste mehaaniliste omaduste näitajaid saab usaldusväärselt ja täpselt määrata ainult otseste metalliteimide abil.

Traditsioonilised metalli mehaaniliste omaduste määramise meetodid standardsete teimikutega (purustav kontroll) nõuavad metalli väljalõikamist suurtes kogustes, mis ei võimalda elementide edaspidist käitamist. Metalli mittepurustavaks kontrolliks töötati välja kaks lõikeseadet miniatuursete katsetükkide väljalõikamiseks, esimene – proovi võtmiseks kontrollitava elemendi välispinnalt, teine – sissepinnalt. Modelleerimine lõplike elementide meetodil näitas, et mikrokatsetüki väljalõikamise tagajärjel moodustunud süvendis tekkinud pingete kontsentratsioon ei suurenda pingeid üle lubatavate ja seega pingete suurenemine elemendi seinas ei ole ohtlik.

Väljatöötatud lõikeseadmeid on edukalt kasutatud Eesti elektrijaamades. Kokku rohkem kui 200 metalliproovi on välja lõigatud aurutorustike, turbiinikorpuste ja katlatrumlite välispinnalt ning turbiinirootorite teljekanali sisepinnalt.

Üheks töö eesmärgiks oli metalli mehaaniliste omaduste määramiseks kasutatava kuulmeetodi (SP) võimaluste analüüs. Selleks viidi läbi rida võrdluskatseid paralleelselt standardsete meetoditega, kus kasutati standardseid silindrilisi teimikuid. Katsetulemuste võrdlus näitas, et tõmbetugevust saab SP meetodil määrata piisava täpsusega, kuid voolavuspiiri määramise täpsus on ebarahuldav. Sama tulemuse andis ka teimiku kuuliga surumise modelleerimine

lõplike elementide meetodil, kusjuures modelleerimise tulemused näitasid väga head kokkulangevust katsetulemustega.

Metalli mehaaniliste omaduste, esmajoones voolavuspiiri, määramiseks töötati välja miniatuursete teimikute tõmbeteimi metoodika. Uue metoodika täpsuse kontrolliks võrreldi sellel meetodil määratud metalli mehaanilisi omadusi samast materjalist valmistatud standardsete silindriliste katseteimikutega teostatud katsete tulemustega. Võrdlusanalüüs näitas tulemuste väga head kokkulangevust, kusjuures tulemuste korduvus oli suur. See viitab uue katsemetoodika usaldusväärsusele ja katseseadme töökindlusele, aga samuti selle meetodi eelistele. Väljatöötatud metoodika on sertifitseeritud Eesti Akrediteerimiskeskuses ja seda on kasutatud AS NEJ seadmete seisundi hindamiseks. Seega on väljatöötatud metoodika juurutatud praktikas.

Põlevkivi tolmpõletamise katelde küttepinnad töötavad rasketes, kõrgetemperatuurilise korrosiooni ja küttepindade perioodilise tuhasadestistest puhastamise, tingimustes. Läbiviidud laboratoorsete ja tööstuslike katsete alusel on leitud neis tingimustes kõige vastupidavam teras Eesti põlevkivikatelde auruülekuumendite valmistamiseks. Remondimahtude ja maksumuse vähendamiseks töötati välja auruülekuumendi torude jääkressursi hindamise metoodika, mis põhineb toruseina jääkpaksuse mõõtmisel ja konkreetset marki terase korrosioonidiagrammil.

Ülalmainitud uuringute tulemused ja väljatöötatud metoodikad on väga olulised energeetikaseadmete metalli olukorra ja jääkressursi hindamisel ning nad on võetud edukalt kasutusele.

Appendix A
ORIGINAL PUBLICATIONS

PAPER I

Tallermo H., Klevtsov I., Bojarinova T., Dedov A. Laboratory tests of high temperature corrosion of steels B-407, X8CrNiNb1613 and X8CrNiMoNb1616 under impact of PF oil shale ash. Oil Shale, 2005, Vol. 22, No. 4S, pp. 467–474.

PAPER II

Tallermo H., Klevtsov I., Bojarinova T., Dedov A. Assessment of Remaining Life of Superheater austenitic Steel Tubes in PF Oil Shale Boilers. Oil Shale, 2006, Vol. 23, No. 3, pp. 267–274.

PAPER III

Dedov A., Klevtsov I., Lausmaa T., Neshumayev D. Method of small samples for assessment of properties of power plant components: sampling devices and stress concentration in dimples. *In:* Proceedings of international conference Baltica VII on Life Management and Maintenance for Power Plants, Helsinki – Stockholm – Helsinki, 12–14 June, 2007, Vol. 2. Helsinki: VTT Technical Research Centre of Finland, pp. 180–192.

PAPER IV

Klevtsov I., Dedov A., Bogolyubova E., Bojarinova T. Significance of direct testing of mechanical properties of power equipment metal. Accepted for publication in Thermal Engineering (in Russian).

Significance of direct testing of mechanical properties of power equipment metal

Klevtsov I.[1], Dedov A.[1], Bogolyubova E.[2], Bojarinova T.[1]

[1]Tallinn University of Technology, Thermal Engineering Department, Tallinn, Estonia
[2]ER Test Service OÜ, Narva, Estonia

Abstract
Long-term exposure at elevated temperatures results in a degradation of the short-term mechanical properties of metal that can cause the deterioration in reliability of power equipment. Therefore, in order to guarantee safe operation of equipment periodic control of the mechanical properties of metal is highly significant. The comparison of mechanical properties values, calculated as a function of metal hardness according to known relations and obtained from the tensile testing of some power plant steels is presented in this paper. On the basis of wide disagreement of calculated and measured data a conclusion about the significance of direct testing of mechanical properties was drawn.

Appendix B
CURRICULUM VITAE

CURRICULUM VITAE

First name	Andrei
Last name	Dedov
Date and place of birth	14.09.1979, Estonia
Citizenship	Estonian
Family status	Married
Contact	Kalevipoja põik 5-63, 13614 Tallinn, Estonia; Telephone: +372 55595453; E-mail: dedov@staff.ttu.ee
Organization	Tallinn University of Technology (TUT), Thermal Engineering Department (TED), Kopli 116, 11712 Tallinn, Estonia
Current position	Researcher

Education

Educational institution	Year of graduation	Education
Tallinn University of Technology	2003	Master degree
Tallinn University of Technology	2001	Bachelor degree
Pähklimäe Gymnasium, Narva	1997	Secondary Education
Tartu School of Exact Sciences	1997	Course in mathematics

Professional Employment

Period	Organisation	Position
2004-present	Tallinn University of Technology, Thermal Engineering Department	Researcher
2002-2004	Tallinn University of Technology, Thermal Engineering Department	Engineer

Language skills

Language	Level
English	average
Estonian	average
Russian	fluent
German	basic skills

Training courses   Course of life extension of basic and auxiliary thermal power plant equipment. St.-Petersburg, Russia, 2006.

Research Interest   Investigations of the metal conditions for estimation of remaining life of steam boiler's and turbine's units. Safe operation of the thermal equipment at power plants.

ELULOOKIRJELDUS

Eesnimi	Andrei
Perekonnanimi	Dedov
Sünniaeg ja –koht	14.09.1979, Estonia
Kodakondsus	Eesti
Perekonnaseis	Abielus
Kontaktandmed	Kalevipoja põik 5-63, 13614 Tallinn, Eesti; Telefon: +372 55595453; E-mail: dedov@staff.ttu.ee
Töökoht	Tallinna Tehnikaülikool, Soojustehnika Instituut, Kopli 116, 11712 Tallinn, Eesti
Ametikoht	Teadur

Hariduskäik

Õppeasutus	Lõpetamise aeg	Haridus
Tallinna Tehnikaülikool	2003	tehnikamagister
Tallinna Tehnikaülikool	2001	tehnikateaduste bakalaureus
Pähklimäe Gümnaasium, Narva	1997	keskharidus
Täpisteaduste kool, Tartu	1997	matemaatika eriala

Teenistuskäik

Töötamise aeg	Organisatsiooni nimetus	Ametikoht
2004-käesoleva ajani	Tallinna Tehnikaülikool, Soojustehnika Instituut	teadur
2002-2004	Tallinna Tehnikaülikool, Soojustehnika Instituut	insener

Keelteoskus

Keel	Tase
Inglisekeel	kesk
Eestikeel	kesk
Venekeel	kõrg
Saksakeel	alg

Täiendõpe	Soojuselektrijaamade põhi- ning abiseadmete ressursi pikendamine, Sankt-Peterburg, Venemaa, 2006.
Teadustöö põhisuunad	Soojuselektrijaamade seadmete metalli seisundi uuringud ja jääkressursi määramine. Soojusseadmete ohutu käitamise tagamine.